הטכניון – מכון טכנולוגי לישראל
Technion – Israel Institute of Technology

ספריות הטכניון
The Technion Libraries

בית הספר ללימודי מוסמכים ע"ש ארווין וג'ואן ג'ייקובס
Irwin and Joan Jacobs Graduate School

Effect of Polarization on Coherent Back Scattering

Research Thesis

In Partial Fulfillment of The

Requirements for the Degree of

Master of Science in Physics

Moshe Diamant

Submitted to the Senate of

the Technion - Israel Institute of Technology

Iyar, 5770 Haifa April 2010

The Research Thesis Was Done Under The Supervision of Prof. Eric Akkermans

in the Faculty of Physics

Contents

List of symbols

λ	Wave length
l_{pol}	Elastic mean free path
γ_e	Interaction strength
G^A	Advanced Green's function
G^R	Retarded Green's function
D	Diffusion constant
$\Gamma(\mathbf{r},\mathbf{r}')$	Structure factor
p_d	Diffuson probability
X_c	Cooperon probability
α	Albedo

List of Figures

List of Tables

Abstract

This work deals with energy conservation in coherent back scattering. Formulated in the mid 1980's, coherent back scattering infers that for a weakly disordered medium (where the elastic mean free path is much greater than the wave length of the incoming radiation) symmetry with respect to time reversal allows for an additional term in the perturbation theory. The effect of this term changes the angular distribution of the scattered intensity. For the case of a semi infinite system, the intensity is doubled at the zero angle direction and the width of the resulting peak is of order $1/kl_e$ where k is the wave number and l_e the elastic mean free path. However this additional term seems to violate energy conservation as the addition to the scattered intensity is not compensated by a decrease in the rest of the reflected intensity (that is, for angles larger than $\frac{1}{kl_e}$). The reason for this turns out to be the omission of other terms in the perturbation series, which contribute to the same order. The inclusion of the aforementioned scattering terms restores the normalization. This was found also experimentally. In this work it is shown that this remains correct when taking into consideration the polarization of the waves.

Introduction

The phenomenon of coherent back scattering [1, 2, 3], which was predicted theoretically in the mid 80's and later observed in many experiments ([4, 5, 6, 7] to name but a few. More references can be found in[8]) is an example of a coherent behavior which exists in a random medium. Such a medium lacks translational symmetry as opposed to lattices used to model systems in condensed matter. One cannot assign a specific configuration to the constituents of the medium (be it a discrete set of scattering bodies, or a continuous function like the refraction index). Instead one can only consider an ensemble of configurations and their statistics.

Coherent effects arise due to the oscillatory nature of a wave . One of the most known examples is the Young double slit experiment, where two coherent sources create an interference pattern. Now suppose we take a large number of sources with random phases and measure the formed interference pattern. It will appear random since the sources are uncorrelated. If we superimpose the average intensity of many such experiments (varying randomly the distance between the slits in each experiment) we find a uniform resulting intensity. The interference terms cancel out and we have the sum of the individual intensities of the sources. Such reasoning lead to the thinking that coherent effects are lost upon averaging.

The picture is more complicated for diffusion and scattering in a random medium. While we can still model each realization of the disorder as a set of scattering sources close to the surface of the medium, much like the variation of the Young experiment above, we can not rule out the existence of constructive interference. The phase of each outgoing wave is determined by the length of the path it traversed inside the medium. If the phase difference of the different scattered amplitudes can be ignored we can use the classical description for the scattered intensity. This result is represented by the arc in figure (1) and described in section 1.4.

The works of Akkermans and Maynard [1] and Golubenstev [9] showed that it is possible to include another scattering process in the intensity calculation. This contribution which was known as the Cooperon is described in section 1.5. One noticeable hallmark of the Cooperon is that for a semi-infinite medium, when the wave is back scattered - that is when the incoming and outgoing waves emerge along the same direction - the scattered intensity is doubled with respect to the classical scattered intensity. The inclusion of the Cooperon however raises a problem. It is known that the contribution of the Diffuson along with the Drude-Boltzmann term[1] is normalized. The contribution of the Cooperon is always positive which seems to violate energy conservation[2].

In spite of this apparent violation of a fundamental principle in physics, we can not ignore many successful experiments which agree with enhancement of the back scattered intensity. The Cooperon (like the Diffuson) are derived using perturbation theory, and as such are only part of the complete description of the scattered intensity. Indeed, there are more terms in the perturbation series [10] which contribute at the same perturbation

[1] See chapter 1

[2] The scattering is elastic and the medium is thick enough so no radiation passes completely though it

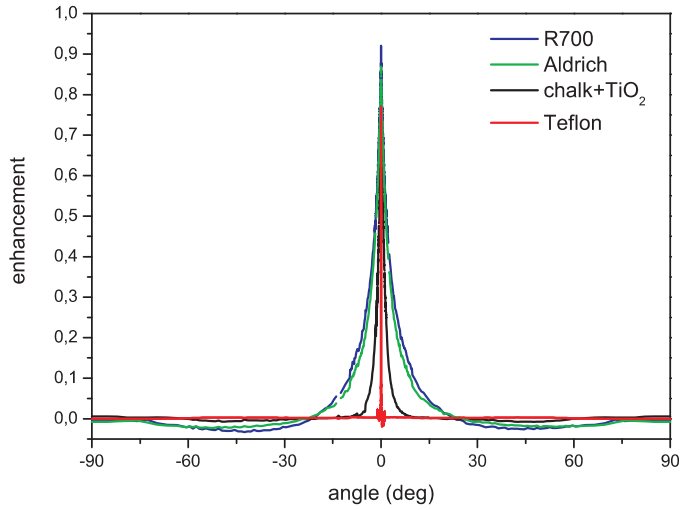

Figure 1: A plot of the angular distribution of a scattered monochromatic wave from different media [7].

order as the Cooperon. In this work we show that the net contributions of the Cooperon and two other terms - known collectively as a dressed Cooperon - is zero.

The outline of this work is as follows. In chapter 1 we introduce the theory of wave diffusion, and the origin of the Diffuson and the Cooperon. We use the results of this chapter to derive the contribution of the Diffuson and the Cooperon to the scattered intensity in chapter 2. Chapters 3 and 4 extend the ideas of the former chapters to include polarization. Finally, in chapter 5 we show how the inclusions of the additional terms in the perturbation series help to restore energy conservation. A comparison of the theoretical result against experimental one is presented at the end of the chapter.

Chapter 1

Probability of Wave Diffusion

Throughout this work we use results of wave diffusion theory. We therefore review them now. We follow the presentation and notation found in chapter 3 and 4 of [8]. The reader is referred to that source for a more detailed presentation.

1.1 Models of disorder

In this section we give a brief description of the Gaussian and Edwards model of disorder which we will make use of later.

The Gaussian model of disorder is one of the simplest yet useful models. Suppose that the disorder potential is a continuous function $V(\mathbf{r})$. The Gaussian model is characterized by

$$\overline{V(\mathbf{r})} = 0 \tag{1.1}$$

$$\overline{V(\mathbf{r})V(\mathbf{r}')} = B(\mathbf{r},\mathbf{r}'). \tag{1.2}$$

where $\overline{\cdots}$ describes averaging over the realizations of the disorder. All higher uneven moments vanish due to (1.1), and higher even moments can be derived from (1.2). We can further simplify the model by assuming that $B(\mathbf{r},\mathbf{r}')$ depends only on the distance such that

$$B(\mathbf{r},\mathbf{r}') = B(\mathbf{r}-\mathbf{r}'). \tag{1.3}$$

Another simplification can be made if we restrict the correlation function to be short ranged. A good choice for such a function is

$$B(\mathbf{r}-\mathbf{r}') = B_0\delta(\mathbf{r}-\mathbf{r}'). \tag{1.4}$$

In the following work we will use (1.4) as our specific correlation function.

A different model, which involves discrete scatterers, was studied for electrons by Edwards in 1958 [11].In this model the disorder potential is

$$V = \sum_{j=1}^{N} v(\mathbf{r}-\mathbf{r}_j). \tag{1.5}$$

In the limit where the scatterers density $n_i = \frac{N}{V}$ approaches infinity, and the potential $v(\mathbf{r})$ is very weak, the Edwards model becomes equivalent to the previous Gaussian model [8], provided we identify

$$B(\mathbf{q}) \quad = \quad n_i v(\mathbf{q})^2 \tag{1.6}$$

where $\mathbf{q}$ is the Fourier variable conjugate of $\mathbf{r}-\mathbf{r}'$. The advantage is that we can solve the problem of discrete scatterers, under the conditions specified above, by using continuous functions which are easier to work with.

1.2 Perturbation theory

In this work we wish to calculate quantities which result from multiple scattering of electromagnetic waves. We work in the limit where the wave length is much greater than the size of the scatterers. This limit is known as the Rayleigh scattering. In this limit the effects of polarization and disorder on the scattering amplitude are independent of each other. This allows us to use the scalar wave approximation and incorporate the polarization later. The electric field intensity in the presence of an arbitrary potential $V(\mathbf{r}) = -k_0^2 \mu(\mathbf{r})$ is described then by the following Helmholtz equation

$$\left[-\triangle - k_0^2 (1+\mu(\mathbf{r}))\right] \psi(\mathbf{r}) \quad = \quad 0 \tag{1.7}$$

where $\mu(\mathbf{r}) = \frac{\delta\varepsilon}{\bar{\varepsilon}}$ is the random variation of the dielectric constant as measured relative to its average value, and k_0 is the wave number of the given monochromatic wave. This can be treated as an eigenvalue problem for the differential operator $\mathscr{L}$ (and $\mathscr{L}_0$ for a free medium)

$$\mathscr{L} \quad = \quad -\triangle + V \tag{1.8}$$

$$\mathscr{L}_0 \quad = \quad -\triangle \tag{1.9}$$

where $\triangle$ is the Laplacian operator. These operators act on functions in $\mathbf{L}^2$ (square integrable) with an inner product

$$\langle \phi | \chi \rangle \quad = \quad \int d\mathbf{r} \phi^*(\mathbf{r}) \chi(\mathbf{r}) \tag{1.10}$$

are self-adjoined and have a complete set of eigenfunctions which form a basis[1] in which we can expand any sufficiently regular function[12]. We can write these operators in the spectral representation

$$\mathscr{L} \quad = \quad \int d\mathbf{n} \lambda_n |\psi_n\rangle\langle\psi_n| \tag{1.11}$$

$$\mathscr{L}_0 \quad = \quad \int d\mathbf{n} k_n |\phi_n\rangle\langle\phi_n| . \tag{1.12}$$

where $|\psi_n\rangle, \lambda_n$ and $|\phi_n\rangle$,k_n are the eigenfunctions and eigenvalues of $\mathscr{L}$ and $\mathscr{L}_0$ respectively and n is a continuous parameters which is used as an index to label the various functions of the basis[12]. A common approach for solving (1.7) is to use the Green's function $G(\mathbf{r},\mathbf{r}',k_0)$ which is the solution of the inhomogeneous equation

$$\left[-\triangle - k_0^2 (1+\mu(\mathbf{r}))\right] G(\mathbf{r},\mathbf{r}',k_0) \quad = \quad \delta(\mathbf{r}-\mathbf{r}') . \tag{1.13}$$

[1] The functions composing this basis are not necessarily square integrable.

In its operator form the Green's function is defined as follows

$$\hat{G} \equiv \frac{1}{k_0^2 - \mathscr{L}} \tag{1.14}$$

and

$$\hat{G}_0 \equiv \frac{1}{k_0^2 - \mathscr{L}_0} \tag{1.15}$$

in a free medium. The Green's operator[2] relates between $\psi(\mathbf{r})$ and $\psi(\mathbf{r}')$

$$\begin{aligned} \left\langle \mathbf{r} \right| \left(k_0^2 - \mathscr{L}\right) \hat{G} \left| \psi \right\rangle &= \langle \mathbf{r} | \psi \rangle \\ \left(k_0^2 - \mathscr{L}_r\right) \int d\mathbf{r}' \left\langle \mathbf{r} \right| \hat{G} |\mathbf{r}'\rangle \left\langle \mathbf{r}' \right| \psi \rangle &= \psi(\mathbf{r}) \\ \left(k_0^2 - \mathscr{L}_r\right) \int d\mathbf{r}' G\left(\mathbf{r}, \mathbf{r}', k_0\right) \psi\left(\mathbf{r}'\right) &= \psi(\mathbf{r}) \end{aligned} \tag{1.16}$$

where $\mathscr{L}_r$ is the differential operator with respect to the variable $\mathbf{r}$ in the spatial representation.

To obtain the Green's function in the spatial representation $G(\mathbf{r}, \mathbf{r}', k_0)$, we start with its spectral representation

$$\begin{aligned} \hat{G} &= \frac{1}{k_0^2 - \mathscr{L}} \\ &= \int dn \frac{|\psi_n\rangle\langle\psi_n|}{k_0^2 - \lambda_n}. \end{aligned} \tag{1.17}$$

$$\begin{aligned} \hat{G}_0 &= \frac{1}{k_0^2 - \mathscr{L}_0} \\ &\int dn \frac{|\phi_n\rangle\langle\phi_n|}{k_0^2 - k_n}. \end{aligned} \tag{1.18}$$

The Green's function is given by

$$G\left(\mathbf{r}, \mathbf{r}', k_0\right) = \left\langle \mathbf{r} \right| \hat{G} \left| \mathbf{r}' \right\rangle$$

$$= \int dn \frac{\langle \mathbf{r} | \psi_n \rangle \langle \psi_n | \mathbf{r}' \rangle}{k_0^2 - \lambda_n} \tag{1.19}$$

$$= \int dn \frac{\psi_n(\mathbf{r}) \psi_n^*(\mathbf{r}')}{k_0^2 - \lambda_n}. \tag{1.20}$$

[2] A similar derivation exist also for the free Green's operator.

We can check now the validity of (1.16)

$$\begin{aligned}
\left(k_0^2-\mathscr{L}_r\right)\int d\mathbf{r}'G\left(\mathbf{r},\mathbf{r}',k_0\right)\psi\left(\mathbf{r}'\right) &= \left(k_0^2-\mathscr{L}_r\right)\int d\mathbf{r}'\int dn\frac{\psi_n\left(\mathbf{r}\right)\psi_n^*\left(\mathbf{r}'\right)}{k_0^2-\lambda_n}\psi\left(\mathbf{r}'\right)\\
&= \int d\mathbf{r}'\int dn\frac{\left(k_0^2-\lambda_n\right)\psi_n\left(\mathbf{r}\right)\psi_n^*\left(\mathbf{r}'\right)}{k_0^2-\lambda_n}\psi\left(\mathbf{r}'\right)\\
&= \int d\mathbf{r}'\left[\int dn\psi_n\left(\mathbf{r}\right)\psi_n^*\left(\mathbf{r}'\right)\right]\psi\left(\mathbf{r}'\right)\\
&= \int d\mathbf{r}'\delta\left(\mathbf{r}-\mathbf{r}'\right)\psi\left(\mathbf{r}'\right)\\
&= \psi\left(\mathbf{r}\right) \qquad (1.21)
\end{aligned}$$

The free Green's function (for the case $\mu\left(\mathbf{r}\right)=0$) has a similar form

$$G_0\left(\mathbf{r},\mathbf{r}',k_0\right) = \int dn\frac{\phi_n\left(\mathbf{r}\right)\phi_n^*\left(\mathbf{r}'\right)}{k_0^2-k_n}. \qquad (1.22)$$

We see that we can express the Green's function through the eigenfunctions and eigenvalues of the corresponding differential operator $\mathscr{L}$. For the free Green's function it is quite easy. The eigenvalue equation for $\mathscr{L}_0$ is

$$\mathscr{L}_0\phi_n = k_n\phi_n \qquad (1.23)$$

whose solutions for a three dimensional infinite space are plane waves $e^{i\mathbf{k}\cdot\mathbf{r}}$ with an eigenvalue k^2. Inserting into (1.22) we find

$$G_0\left(\mathbf{r},\mathbf{r}',k_0\right) = \int\frac{e^{i\mathbf{k}\cdot\left(\mathbf{r}-\mathbf{r}'\right)}}{k_0^2-k^2-i\varepsilon}d\mathbf{k}. \qquad (1.24)$$

The added imaginary part was inserted to ensure convergence. Performing the angular integration we are left with

$$G_0\left(\mathbf{r},\mathbf{r}',k_0\right) = \int_0^\infty\frac{k}{i\left|\mathbf{r}-\mathbf{r}'\right|}\frac{e^{-ik\left|\mathbf{r}-\mathbf{r}'\right|}-e^{ik\left|\mathbf{r}-\mathbf{r}'\right|}}{k_0^2-k^2-i\varepsilon}dk.$$

Since the integrand is even we can write

$$G_0\left(\mathbf{r},\mathbf{r}',k_0\right) = \int_{-\infty}^\infty\frac{k}{2i\left|\mathbf{r}-\mathbf{r}'\right|}\frac{e^{-ik\left|\mathbf{r}-\mathbf{r}'\right|}-e^{ik\left|\mathbf{r}-\mathbf{r}'\right|}}{k_0^2-k^2-i\varepsilon}dk.$$

We solve this integral in the complex plane

$$\begin{aligned}
G_0\left(\mathbf{r},\mathbf{r}',k_0\right) &= \oint\frac{k}{2i\left|\mathbf{r}-\mathbf{r}'\right|}\frac{e^{-ik\left|\mathbf{r}-\mathbf{r}'\right|}-e^{ik\left|\mathbf{r}-\mathbf{r}'\right|}}{k_0^2-k^2-i\varepsilon}dk\\
&= \oint\frac{k}{2i\left|\mathbf{r}-\mathbf{r}'\right|}\frac{e^{-ik\left|\mathbf{r}-\mathbf{r}'\right|}-e^{ik\left|\mathbf{r}-\mathbf{r}'\right|}}{\left(k+k_0+i\varepsilon\right)\left(k_0-k-i\varepsilon\right)}dk.
\end{aligned}$$

This integral has a pole in the upper and lower halves of the complex plane. Using the residue theory we have

$$2\pi i G_0^{R,A}\left(\mathbf{r},\mathbf{r}',k_0\right) = I_1 - I_2$$

where I_1 has a contour around the upper half of the complex plane, and I_2 around the lower half.

$$\begin{aligned} I_1 &= \oint_{\Im k\geq 0} \frac{k}{2i\left|\mathbf{r}-\mathbf{r}'\right|} \frac{e^{ik\left|\mathbf{r}-\mathbf{r}'\right|}}{\left(k+k_0+i\varepsilon\right)\left(k_0-k-i\varepsilon\right)} dk \\ I_2 &= \oint_{\Im k\leq 0} \frac{k}{2i\left|\mathbf{r}-\mathbf{r}'\right|} \frac{-e^{-ik\left|\mathbf{r}-\mathbf{r}'\right|}}{\left(k+k_0+i\varepsilon\right)\left(k_0-k-i\varepsilon\right)} dk \end{aligned}$$

Performing the integration we have

$$\begin{aligned} I_1 &= \frac{k}{2i\left|\mathbf{r}-\mathbf{r}'\right|} \frac{e^{ik\left|\mathbf{r}-\mathbf{r}'\right|}}{\left(k+k_0+i\varepsilon\right)}\Big|_{k=k_0+i\varepsilon} \\ &= \frac{k_0}{2i\left|\mathbf{r}-\mathbf{r}'\right|} \frac{e^{i(k_0+i\varepsilon)\left|\mathbf{r}-\mathbf{r}'\right|}}{2\left(k_0+i\varepsilon\right)} \\ &\underset{\varepsilon\to 0}{=} \frac{1}{i\left|\mathbf{r}-\mathbf{r}'\right|} \frac{e^{ik_0\left|\mathbf{r}-\mathbf{r}'\right|}}{4} \end{aligned}$$

and similarly

$$I_2 = \frac{-i}{\left|\mathbf{r}-\mathbf{r}'\right|} \frac{e^{ik_0\left|\mathbf{r}-\mathbf{r}'\right|}}{4}$$

The free Green's function is then

$$G_0^A\left(\mathbf{r},\mathbf{r}',k_0\right) = -\frac{1}{\left|\mathbf{r}-\mathbf{r}'\right|} \frac{e^{ik_0\left|\mathbf{r}-\mathbf{r}'\right|}}{4\pi}.$$

If we had chosen the opposite sign before $i\varepsilon$ in (1.24) we would get

$$G_0^R\left(\mathbf{r},\mathbf{r}',k_0\right) = -\frac{1}{\left|\mathbf{r}-\mathbf{r}'\right|} \frac{e^{-ik_0\left|\mathbf{r}-\mathbf{r}'\right|}}{4\pi}.$$

The two solutions

$$G_0^{R,A}\left(\mathbf{r},\mathbf{r}',k_0\right) = -\frac{1}{\left|\mathbf{r}-\mathbf{r}'\right|} \frac{e^{\mp ik_0\left|\mathbf{r}-\mathbf{r}'\right|}}{4\pi} \tag{1.25}$$

the retarded Green's function with the minus sign in the exponent and the advanced Green's function with the plus sign in the exponent describe waves propagating in opposite directions to each other.

It is possible to solve the eigenvalue equation for the full Green's function $G\left(\mathbf{r},\mathbf{r}',k_0\right)$ using the solution for the free Green's function. Noting that

$$\hat{G} = \frac{1}{\hat{G}_0^{-1} - V} \tag{1.26}$$

we find an iterative equation for the Green's operator

$$\hat{G} = \hat{G}_0 + \hat{G}_0 V \hat{G} \tag{1.27}$$

which allows us to express the full Green's function using the potential term and the free Green's function.

In real space, using the basis $|\phi_n>$, defined in (1.23), (1.27) reads

$$\begin{aligned} G(\mathbf{r},\mathbf{r}',k_0) &= G_0(\mathbf{r},\mathbf{r}',k_0) - k_0^2 \int d\mathbf{r}_1 G_0(\mathbf{r},\mathbf{r}_1,k_0)\,\mu(\mathbf{r}_1)\,G_0(\mathbf{r}_1,\mathbf{r}',k_0) + \\ & k_0^4 \int d\mathbf{r}_1 d\mathbf{r}_2 G_0(\mathbf{r},\mathbf{r}_1,k_0)\,\mu(\mathbf{r}_1)\,G_0(\mathbf{r}_1,\mathbf{r}_2,k_0)\,\mu(\mathbf{r}_2)\,G_0(\mathbf{r}_2,\mathbf{r}',k_0)\ldots. \end{aligned} \tag{1.28}$$

When averaging over the disorder in (1.28) only terms with an even number of $k_0^2\mu(\mathbf{r})$ in them will remain. From (1.2) each pair $k_0^2\mu(\mathbf{r})\,k_0^2\mu(\mathbf{r}')$ will contribute $B(\mathbf{r}-\mathbf{r}')$ after averaging. The averaging restores translational invariance which prompts us to write the averaged Green's function in momentum space as the following series[3]

$$\begin{aligned} \overline{G}(\mathbf{k},k_0) &= G_0(\mathbf{k}) + \frac{1}{\Omega}\sum_{\mathbf{q}} B(\mathbf{q})\,G_0(\mathbf{k})\,G_0(\mathbf{k}-\mathbf{q})\,G_0(\mathbf{k}) + \\ & \frac{1}{\Omega^2}\sum_{\mathbf{q}}\sum_{\mathbf{q}'} G_0(\mathbf{k})\,B_0(\mathbf{q})\,G_0(\mathbf{k}-\mathbf{q})\,G_0(\mathbf{k})\,B_0(\mathbf{q})\,G_0(\mathbf{k}-\mathbf{q}')\,G_0(\mathbf{k}) + \ldots. \end{aligned} \tag{1.29}$$

where Ω is the volume of the system.

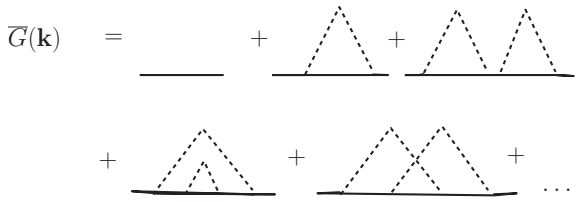

Figure 1.1: The average Green's function in momentum space. The first three diagrams correspond to the first three terms in (1.29)

Consider now the double sum in (1.29) (the third diagram in figure (1.1)) . It can be factored into a product of two sums

$$\sum_{\mathbf{q}}\sum_{\mathbf{q}'} G_0(\mathbf{k})\,B_0(\mathbf{q})\,G_0(\mathbf{k}-\mathbf{q})\,G_0(\mathbf{k})\,B_0(\mathbf{q})\,G_0(\mathbf{k}-\mathbf{q}')\,G_0(\mathbf{k}) = G_0(\mathbf{k})\left[\sum_{\mathbf{q}} G_0(\mathbf{k})\,B_0(\mathbf{q})\,G_0(\mathbf{k}-\mathbf{q})\right]^2. \tag{1.30}$$

We can divide all the terms in (1.29) into two types. Those which can be factorized into a product of other terms, and those which can not. In the diagrammatic description the former are known as reducible or separable and the later as irreducible. The sum of all irreducible diagrams is called the self-energy and designated by $\Sigma(\mathbf{k})$.

[3] Note that the second term in (1.28) cancels after the averaging, and the second term in (1.29) comes from the third one in (1.28).

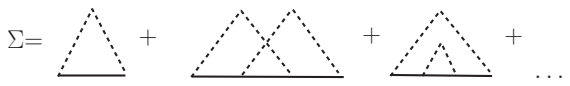

Figure 1.2: The self energy Σ is composed of all the irreducible diagrams. The first diagram corresponds to Σ_1.

(1.29) can be written in the following way

$$\overline{G}(\mathbf{k},k_0) = G_0(\mathbf{k}) + G_0(\mathbf{k})\Sigma_1(\mathbf{k})G_0(\mathbf{k}) + G_0(\mathbf{k})\Sigma_1(\mathbf{k})G(\mathbf{k})\Sigma_1 G_0(\mathbf{k}) + \ldots$$

In a similar fashion we can construct all separable terms from products of the self energy and write the series (1.29) as

$$\begin{aligned}\overline{G}(\mathbf{k},k_0) &= G_0(\mathbf{k}) + G_0(\mathbf{k})\sum_{n=1}^{\infty}\left[\Sigma(\mathbf{k})G_0(\mathbf{k})\right]^n \\ &= G_0(\mathbf{k}) + G_0(\mathbf{k})\Sigma(\mathbf{k})\overline{G}(\mathbf{k},k_0).\end{aligned} \tag{1.31}$$

From (1.31) we obtain the average Green's function for a scalar wave in a disordered medium

$$\overline{G}^{R,A}(\mathbf{k},k_0) = \frac{1}{k_0^2 - k^2 - \Sigma^{R,A}(\mathbf{k})}. \tag{1.32}$$

The first term Σ_1 is

$$\Sigma_1^{R,A}(\mathbf{k}) = \frac{1}{\Omega}\sum_{\mathbf{q}} B(\mathbf{q})G_0(\mathbf{k}-\mathbf{q}). \tag{1.33}$$

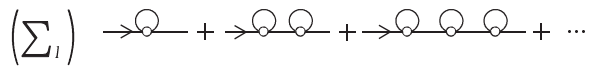

Figure 1.3: By retaining only the first term in the self energy the averaged Green's function is the sum of the following diagrams [8].

We are interested mostly in the imaginary part of Σ_1 which determines how the wave amplitude is affected by the disorder (the real part introduces a shift to the wave frequencies which is equal for all frequencies). Using the following relation between the Green's function and the density of states per unit volume

$$\rho_0(k_0) = -\frac{2k_0}{\pi\Omega c}\sum_{\mathbf{k}'}\Im G_0(\mathbf{k}') = \sum_{\mathbf{k}'}\delta\left(\omega_0(k_0) - \omega(\mathbf{k}')\right) \tag{1.34}$$

The imaginary part of the first term of the self energy can be written as

$$\begin{aligned}\Im\Sigma_1^{R,A}(\mathbf{k}) &= -\frac{\pi c\gamma_e}{2k_0}\rho_0(k_0)\\ &= -\frac{\gamma_e k_0}{4\pi}\end{aligned} \tag{1.35}$$

where the density of states of a free wave $\rho_0(k_0)=\frac{k_0^2}{2\pi^2 c}$ was used and $\gamma_e=\langle B(\mathbf{q})\rangle$ is the angular average over the correlation function[4] (1.6). We define now a length scale, the elastic mean free path l_e

$$\frac{1}{l_e} = -\frac{1}{k_0}\Im\Sigma_1^R(\mathbf{k}). \tag{1.36}$$

As for the higher terms in Σ, in a three dimensional system they are of order $\frac{1}{k_0 l_e}$ [8] and in the limit $k_0 l_e \gg 1$, also known as the weak disorder limit they are negligible. The justification for using this limit is as follows. In the limit of high densities and weak potential the Edwards model coincide with the Gaussian model which we use. The individual scatterings in the Edwards model can be described using the Born approximation where the scattering cross section can be related to the correlation function (1.6) through

$$\gamma_e = \langle B(\mathbf{q})\rangle = 4\pi n_i\sigma. \tag{1.37}$$

From (1.36) we have

$$\frac{1}{l_e} = \frac{\gamma_e}{4\pi}. \tag{1.38}$$

Combining the above result we have

$$\frac{1}{l_e} = n_i\sigma. \tag{1.39}$$

For Rayleigh scattering in a homogeneous medium the cross section is proportional to $k_0^4\mho^2$, where $\mho$ here is the size of the scatterer. Inserting into (1.39) we have

$$\frac{1}{k_0 l_e} \propto \frac{\mho}{\lambda^3}(\mho n_i) \ll 1 \tag{1.40}$$

where on the right hand side we have a quantity which is much less than 1 according to the model we use (we assume the wave length is much larger than the size of the scatterers).

In the weak disorder limit we can see why l_e is called the elastic mean free path. Inserting (1.36) into (1.32) (and ignoring the real part of Σ) the averaged Green's function in momentum space is

$$\overline{G}^{R,A}(\mathbf{k},k_0) = \frac{1}{k_0^2-k^2\pm i\frac{k_0}{l_e}}. \tag{1.41}$$

The added imaginary term in the denominator is responsible for an exponential decrease of the average Green's function in real space

$$\overline{G}^{R,A}(\mathbf{r},\mathbf{r}',k_0) = -\frac{1}{4\pi}\frac{e^{\pm ik_0|\mathbf{r}-\mathbf{r}'|}}{|\mathbf{r}-\mathbf{r}'|}e^{-\frac{|\mathbf{r}-\mathbf{r}'|}{2l_e}}. \tag{1.42}$$

We can thus consider l_e as a mean distance between scattering.

[4] For the correlation function (1.4) $\gamma_e = B_0$.

1.3 Definition of wave diffusion probability

Consider a Gaussian wave packet with an average frequency ω_0 and width σ, centered near a point $\mathbf{r}$ at time t. We define probability function $p(\mathbf{r},\mathbf{r}',t)$ to find a wave packet at a point $\mathbf{r}'$ in a later time t'. The Fourier transform with respect to time of this correlation function is given by

$$p(\mathbf{r},\mathbf{r}',\omega) \equiv \frac{4\pi}{c}\overline{G^R_{\omega_0}(\mathbf{r},\mathbf{r}')\,G^A_{\omega_0-\omega}(\mathbf{r}',\mathbf{r})} \tag{1.43}$$

where ω is the Fourier conjugate of $t'-t$. We use the ρ_0 , the density of modes of a free wave. It differs from the true density of modes in the medium by correction of the order $(k_0 l_e)^{-2}$ which is negligible in the weak disorder limit. If we confine ourselves to a small frequency band $(\omega \ll \sigma)$ where the density of states also changes slowly we can consider ρ_0 as independent of the frequency and further simplify the calculations. The probability function (1.43) obeys the following energy conservation condition

$$\int p(\mathbf{r},\mathbf{r}',\omega)\,\mathrm{d}\mathbf{r}' = \frac{i}{\omega}. \tag{1.44}$$

A simple approximation for (1.43) is the Drude-Boltzmann approximation, for which the average of a product of Green's functions is replaced by a product of averages,

$$p_0(\mathbf{r},\mathbf{r}',\omega) = \frac{4\pi}{c}\overline{G}^R_{\omega_0}(\mathbf{r},\mathbf{r}')\,\overline{G}^A_{\omega_0-\omega}(\mathbf{r}',\mathbf{r}). \tag{1.45}$$

Using (1.42) and expanding $k_0(\omega_0)-k_0(\omega_0-\omega)\approx\omega\frac{\partial k_0}{\partial\omega}=\frac{\omega}{v}$ where v is the group velocity we obtain

$$p_0(\mathbf{r},\mathbf{r}',k_0) = \frac{1}{4\pi c|\mathbf{r}-\mathbf{r}'|^2}e^{i|\mathbf{r}-\mathbf{r}'|k_0}e^{-\frac{|\mathbf{r}-\mathbf{r}'|}{l_e}}. \tag{1.46}$$

This approximation describes the probability of a diffusion from $\mathbf{r}$ to $\mathbf{r}'$ with no scattering. When calculating the total probability for such a process we find that it is not normalized,

$$\int p_0(\mathbf{r},\mathbf{r}',t)\,d\mathbf{r}' \propto \Theta(t)\,e^{-\frac{t}{\tau_e}} \tag{1.47}$$

where the elastic mean free time between scattering is $\tau_e=\frac{l_e}{v}$. The reason is that (1.46) does not take into consideration multiple scattering. Such a process will be described in the following section.

1.4 The Diffuson

To calculate (1.43) we must consider all possible scattering sequences between the initial point $\mathbf{r}$ and the final point $\mathbf{r}'$ with average frequency ω_0, for all possible configurations of the scattering locations. The Green's function which describes the amplitude of such propagation is

$$G(\mathbf{r},\mathbf{r}',k_0) = \sum_{N=1}^{\infty}\sum\left|\mathscr{A}(\mathbf{r},\mathbf{r}',\mathscr{C}_N)\right|e^{ik_0\mathscr{L}_N} \tag{1.48}$$

where the first sum corresponds to the number of scattering events in the sequence. The second sum is over all possible ordering of the scattering events positions in the sequence. $\mathscr{A}(\mathbf{r},\mathbf{r}',\mathscr{C}_N)$ is the amplitude associated with a unique sequence and $k_0\mathscr{L}_N$ is the accumulated phase gained along a scattering trajectory of length $\mathscr{L}$. A typical contribution to the sum is shown in figure (1.4)

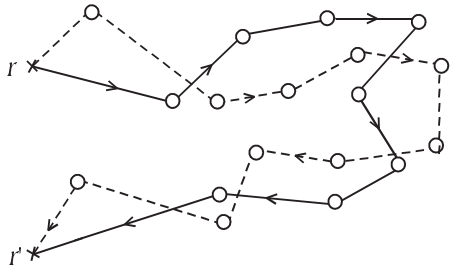

Figure 1.4: Two possible scattering trajectories which contributes to the Green's function $G(\mathbf{r},\mathbf{r}',k_0)$. The two trajectories have a different number of scattering events, none of which shared by both trajectories [8].

To see where such an expression comes from we turn to equation (1.28). Consider the second term on the right hand side. It involves two scattering events located at the points $\mathbf{r}_1$ and $\mathbf{r}_2$. The integration in (1.28) corresponds to the inner sum in (1.48) which runs over all scattering sequences, their positions and order. The outer sum corresponds to the different terms on the right hand side of (1.28).

In the limit of weak disorder, that is when the elastic mean free path l_e is much greater than the wave length $\lambda = \frac{2\pi}{k_0}$ the short range of the potential in (1.4) has the following consequences on the average $\overline{G^R G^A}$.

1. Only trajectories of G^R and G^A with the same ensemble of scattering events are kept. If the ensembles are different we have terms where we need to average over $V(\mathbf{r}_1)V(\mathbf{r}_2)$ with $\mathbf{r}_1 \neq \mathbf{r}_2$, which in our model is zero. See figure 1.5

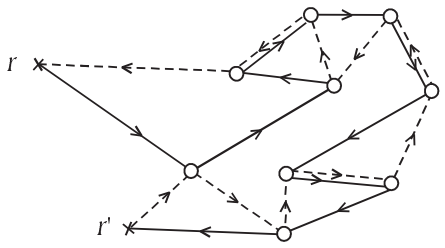

Figure 1.5: Trajectories which share the same ensemble of scattering, yet reaching the different scattering events in a different order. The two trajectories accumulate a different phase and interfere with each other destructively [8].

2. Of those trajectories which fulfill the above criterion we keep those where both G^R and G^A propagate along the sequence of scatterers in the same order. Since the elastic mean free path[5] is much greater than the wave length, trajectories with different order of scattering events will have a phase difference greater than 2π which leads to destructive interference. See figure 1.6.

In this approximation, called the Diffuson approximation the entire procedure is made up of three stages

1. An incoming wave which makes its way to the first scattering event.
2. A sequence of scattering along a path which obeys the restrictions above.
3. An outgoing wave from the last scattering event.

The entire scattering process between the points $\mathbf{r}$ and $\mathbf{r}'$ can be described by the following expression

$$p_d\left(\mathbf{r},\mathbf{r}',\omega\right) = \frac{4\pi}{c}\int d\mathbf{r}_1 d\mathbf{r}_2 \overline{G}^R_{\omega_0}\left(\mathbf{r},\mathbf{r}_1\right)\overline{G}^A_{\omega_0-\omega}\left(\mathbf{r}_1,\mathbf{r}\right)\Gamma_\omega\left(\mathbf{r}_1,\mathbf{r}_2\right)\overline{G}^R_{\omega_0}\left(\mathbf{r}_2,\mathbf{r}'\right)\overline{G}^A_{\omega_0-\omega}\left(\mathbf{r}',\mathbf{r}_2\right). \quad (1.49)$$

The terms $\overline{G}^R_{\omega_0}\left(\mathbf{r},\mathbf{r}_1\right)\overline{G}^A_{\omega_0-\omega}\left(\mathbf{r}_1,\mathbf{r}\right)$ and $\overline{G}^R_{\omega_0}\left(\mathbf{r}_2,\mathbf{r}'\right)\overline{G}^A_{\omega_0-\omega}\left(\mathbf{r}',\mathbf{r}_2\right)$ refer to the incoming and outgoing wave respectively, where $\overline{G}^{R,A}$ is the averaged Green's function of the Helmholtz equation, which for a medium whose dimension L is much greater than the elastic mean free path, is given by (1.42).

The second stage describes a scattering sequence between the point $\mathbf{r}$ and the point $\mathbf{r}'$ with any given non negative integer number of intermediate scattering events. It is called the structure factor or vertex function,

[5] One should understand that the elastic mean free path exist only after the averaging. However, it is still very unlikely for two trajectories with a different order of scattering to accumulate the same phase.

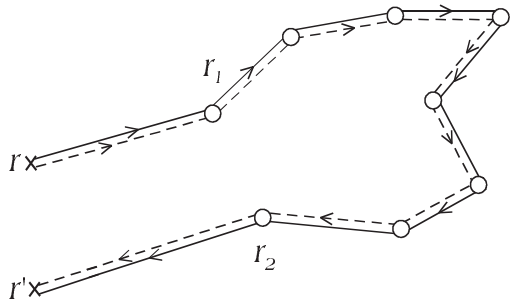

Figure 1.6: Two trajectories which propagate along the same sequence of scattering. They contribute to the incoherent scattering term.[8]

designated here as $\Gamma_\omega(\mathbf{r}_1,\mathbf{r}_2)$ and defined through (1.49). With only a single intermediate scattering event, the scattering process is given by

$$p_d(\mathbf{r},\mathbf{r}',\omega) = \frac{4\pi}{c}\int d\mathbf{r}_1 \overline{G}^R_{\omega_0}(\mathbf{r},\mathbf{r}'')\,\overline{G}^A_{\omega_0-\omega}(\mathbf{r}_1,\mathbf{r})\,\overline{V}(\mathbf{r}_1)\,\overline{G}^R_{\omega_0}(\mathbf{r}_1,\mathbf{r}')\,\overline{G}^A_{\omega_0-\omega}(\mathbf{r},\mathbf{r}_1) \tag{1.50}$$

which gives zero due to (1.1). This will be true also for any sequence of an uneven number of scattering events. We next consider a scattering process with two intermediate scattering events at $\mathbf{r}_1$ and $\mathbf{r}_2$.

$$\begin{aligned} p_d(\mathbf{r},\mathbf{r}',\omega) &= \frac{4\pi}{c}\int d\mathbf{r}_1 d\mathbf{r}_2 \overline{G}^R_{\omega_0}(\mathbf{r},\mathbf{r}_1)\,\overline{G}^A_{\omega_0-\omega}(\mathbf{r}_2,\mathbf{r})\,\overline{V(\mathbf{r}_1)V(\mathbf{r}_2)}\,\overline{G}^R_{\omega_0}(\mathbf{r}_2,\mathbf{r}')\,\overline{G}^A_{\omega_0-\omega}(\mathbf{r},\mathbf{r}_2) \\ &= \frac{4\pi}{c}\int d\mathbf{r}_1 d\mathbf{r}_2 \overline{G}^R_{\omega_0}(\mathbf{r},\mathbf{r}_1)\,\overline{G}^A_{\omega_0-\omega}(\mathbf{r}_2,\mathbf{r})\,\gamma_e\delta(\mathbf{r}_1-\mathbf{r}_2)\,\overline{G}^R_{\omega_0}(\mathbf{r}_1,\mathbf{r}')\,\overline{G}^A_{\omega_0-\omega}(\mathbf{r}',\mathbf{r}_2) \\ &= \frac{4\pi}{c}\gamma_e\int d\mathbf{r}_1 d\mathbf{r}_2 \delta(\mathbf{r}_1-\mathbf{r}_2)\,\overline{G}^R_{\omega_0}(\mathbf{r},\mathbf{r}_1)\,\overline{G}^A_{\omega_0-\omega}(\mathbf{r}_1,\mathbf{r})\,\overline{G}^R_{\omega_0}(\mathbf{r}_1,\mathbf{r}')\,\overline{G}^A_{\omega_0-\omega}(\mathbf{r}',\mathbf{r}_1)\,. \end{aligned} \tag{1.51}$$

Comparing this result to (1.49) we see that for a sequence two scattering event

$$\Gamma_\omega(\mathbf{r}_1,\mathbf{r}_2) = \gamma_e\delta(\mathbf{r}_1-\mathbf{r}_2)\,. \tag{1.52}$$

Since in our model all the scattering events are independent we can construct Γ_ω by repeatedly inserting additional scattering events. We have the following integral equation for the structure factor

$$\Gamma_\omega(\mathbf{r}_1,\mathbf{r}_n) = \gamma_e\delta(\mathbf{r}_1-\mathbf{r}_n)+\gamma_e\int d\mathbf{r}_2\overline{G}^R_{\omega_0}(\mathbf{r}_1,\mathbf{r}_2)\,\overline{G}^A_{\omega_0-\omega}(\mathbf{r}_2,\mathbf{r}_1)\,\Gamma_\omega(\mathbf{r}_2,\mathbf{r}_n)\,. \tag{1.53}$$

The product of average Green's function in (1.49) and (1.53) is simply the Drude-Boltzman term (1.45). Inserting it we write p_d as

$$p_d\left(\mathbf{r},\mathbf{r}',\omega\right) = \frac{c}{4\pi}\int d\mathbf{r}_1 d\mathbf{r}_n p_0\left(\mathbf{r},\mathbf{r}_1\right)\Gamma_\omega\left(\mathbf{r}_1,\mathbf{r}_n\right)p_0\left(\mathbf{r}_n,\mathbf{r}'\right) \tag{1.54}$$

and

$$\Gamma_\omega\left(\mathbf{r}_1,\mathbf{r}_n\right) = \gamma_e\delta\left(\mathbf{r}_1-\mathbf{r}_n\right)+\frac{c}{4\pi}\gamma_e\int d\mathbf{r}_2\Gamma_\omega\left(\mathbf{r}_2,\mathbf{r}_n\right)p_0\left(\mathbf{r}_1,\mathbf{r}_2\right). \tag{1.55}$$

The sum of the two expressions $p_d\left(\mathbf{r},\mathbf{r}'\right)+p_0\left(\mathbf{r},\mathbf{r}'\right)$ is normalized. See section (1.6) for a more convenient calculation in momentum space.

In the weak disorder limit (1.54) can be related to the solution of a classical diffusion equation. This approximation is valid only for a large number of collisions[6] and when the structure factor varies a little on a scale of l_e ($l_e\nabla\Gamma_{r_n}\left(\mathbf{r}_1,\mathbf{r}_n\right)\ll\Gamma\left(\mathbf{r}_1,\mathbf{r}_n\right)-\Gamma\left(\mathbf{r}_1,\mathbf{r}'\right)$, $|\mathbf{r}_n-\mathbf{r}'|\approx l_e$). This is also known as the diffusive limit. When these conditions are fulfilled we find that

$$\left(-i\omega-D\triangle_{\mathbf{r}_n}\right)\Gamma_\omega\left(\mathbf{r}_1,\mathbf{r}_n\right) = \frac{\gamma_e}{\tau_e}\delta\left(\mathbf{r}_1-\mathbf{r}_n\right) \tag{1.56}$$

$$\left(-i\omega-D\triangle_{\mathbf{r}'}\right)p_d\left(\mathbf{r},\mathbf{r}',\omega\right) = \delta\left(\mathbf{r}-\mathbf{r}'\right) \tag{1.57}$$

where D is the diffusion constant defined as

$$D=\frac{vl_e}{3} \tag{1.58}$$

in a three dimensional system and v the group velocity of the wave which was derived in (1.46). The solution of the diffusion equation are refereed to as the probability to propagate from a point $\mathbf{r}$ at time t to a point $\mathbf{r}'$ at time t'.

1.5 The Cooperon

While the combination of the Drude-Boltzmann term (1.45) and the Diffuson (1.54) is normalized[7]

$$\int d\mathbf{r}'\left(p_0\left(\mathbf{r},\mathbf{r}',\omega\right)+p_d\left(\mathbf{r},\mathbf{r}',\omega\right)\right)=1$$

we must remember that (1.48) is not a complete explicit expression of $p\left(\mathbf{r},\mathbf{r}',\omega\right)$. We demonstrate now that there exist other scattering processes which contribute to the diffusion probability. Such a scattering process can be constructed by reversing the scattering sequence of one of the propagating amplitudes as shown in diagram (b) of figure (1.7). The trajectory's length remains the same, and if the system possesses time reversal symmetry[8] the same phase $k\mathscr{L}_N$ will be accumulated by both propagating amplitudes. Such a system will have the property

$$G^{R,A}\left(r,r'\right) = G^{R,A}\left(r',r\right). \tag{1.59}$$

[6] The exact solution of (1.54) and (1.55) for an infinite medium can be calculated. It can be shown to be a solution of a classical diffusion equation up to exponentially small corrections. When $|\mathbf{r}-\mathbf{r}'|\approx l_e$ the difference is about 0.03. See appendix 5.1 in reference[8].

[7] This will be demonstrated in the next section.

[8] See Appendix 2.2 in reference [8].

Notice that for the Diffuson the initial and final point are identical for both amplitude. However, they need not be so for if we reverse one of the amplitudes, as depicted in diagram (d) in figure 1.7. We can write the probability for such a contribution starting with (1.49) and interchanging the coordinates of the advanced Green's functions

$$X_c\left(\mathbf{r},\mathbf{r}',\omega\right) = \frac{1}{2\pi\rho_0}\int d\mathbf{r}_1 d\mathbf{r}_2 \overline{G}^R_E\left(\mathbf{r},\mathbf{r}_1\right)\overline{G}^A_{E-\omega}\left(\mathbf{r}_2,\mathbf{r}\right)\Gamma'_\omega\left(\mathbf{r}_1,\mathbf{r}_2\right)\overline{G}^R_E\left(\mathbf{r}_2,\mathbf{r}'\right)\overline{G}^A_{E-\omega}\left(\mathbf{r}',\mathbf{r}_1\right) \quad (1.60)$$

This process is known as the Cooperon[8], or the maximally crossed diagram.

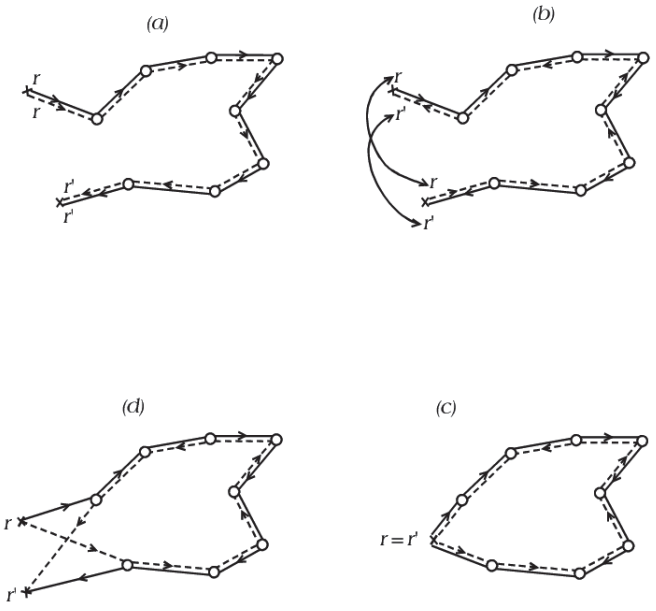

Figure 1.7: a) The Diffuson. b) Reversal of one of the trajectories. c) If $\mathbf{r}$ *and* $\mathbf{r}'$ *coincide then the phase difference cancels out. d) If* $\mathbf{r}$ *and* $\mathbf{r}'$ *differ there is a phase difference between the two propagating amplitudes which diminishes this contribution greatly.[8]*

If the structure factor varies slowly on a scale l_e, as we assumed for the Diffuson, it can be taken outside the integral and the Cooperon becomes

$$X_c\left(\mathbf{r},\mathbf{r}',\omega\right) = \frac{\Gamma'_\omega\left(\mathbf{r},\mathbf{r}'\right)}{2\pi\rho_0\gamma_e^2}\left[\gamma_e\int d\mathbf{r}_1 \bar{G}^R_E\left(\mathbf{r},\mathbf{r}_1\right)\bar{G}^A_E\left(\mathbf{r}',\mathbf{r}_1\right)\right]^2. \quad (1.61)$$

We now consider the resulting structure factor $\Gamma'_{\omega}(\mathbf{r}_1,\mathbf{r}_n)$ and how it changes under the reversal of the scattering order. Since the structure factor is composed of products of averaged Green's functions (see (1.55) and (1.53)) which are invariant under the exchange $\mathbf{r}_1 \leftrightarrow \mathbf{r}_n$ for a translational invariant system, the structure factor is invariant under time reversal of the trajectory

$$\Gamma'_{\omega}(\mathbf{r}_1,\mathbf{r}_2) = \Gamma_{\omega}(\mathbf{r}_1,\mathbf{r}_2). \tag{1.62}$$

For $\mathbf{r} = \mathbf{r}'$ in (1.60) We obtain

$$X_c(\mathbf{r},\mathbf{r},\omega) \quad = \quad p_d(\mathbf{r},\mathbf{r},\omega). \tag{1.63}$$

The Cooperon contribution is equal to the Diffuson contribution when the scattering is along a closed trajectory. When $\mathbf{r} \neq \mathbf{r}'$ the scattered wave and its conjugate will reach each point with a phase difference, since they propagate along different paths. By summing over disorder, that is, summing up the contributions of all the amplitudes, all sequence for which $\mathbf{r} \neq \mathbf{r}'$ will contribute amplitudes with a varying phase which will eventually cancel out. Only trajectories for which $\mathbf{r}$ and $\mathbf{r}'$ are sufficiently close will remain. In three dimensions we find[8] that

$$X_c\left(\mathbf{r},\mathbf{r}',\omega\right) \quad = \quad X_c(\mathbf{r},\mathbf{r},\omega)\frac{\sin^2(k_0R)}{k_0^2R^2}e^{-\frac{R}{l_e}} \tag{1.64}$$

where $\mathbf{R} = |\mathbf{r}-\mathbf{r}'|$. The contribution of the Cooperon decreases exponentially as $\mathbf{r}$ and $\mathbf{r}'$ are further apart (as in sub-figure (d) in figure (1.7)).

1.6 Diffusion in momentum space

The averaging over disorder brings translational invariance (through (1.4)). We utilize it by switching to momentum space. We present first the Fourier transform of the Drude-Boltzmann term (1.45) for a wave packet with an average frequency ω_0

$$p_0(\mathbf{q},\omega) = \frac{1}{2\pi\rho_0\Omega}\sum_k \overline{G}^R_{\omega_0}(\mathbf{q})\,\overline{G}^A_{\omega_0-\omega}(\mathbf{k}-\mathbf{q}) \tag{1.65}$$

where Ω is the volume of the medium, and $\mathbf{q}$ is the Fourier conjugate of $|\mathbf{r}-\mathbf{r}'|$. This expression can be calculated in the limit of weak scattering (when $ql_e \ll 1$, that is when the two amplitudes propagate in the same direction, not to be confused with the condition for weak disorder $k_0 l_e \gg 1$)

$$p_0(q,\omega) \cong \tau_e\left(1+i\tau_e\omega - Dq^2\tau_e\right). \tag{1.66}$$

1.6.1 The Diffuson

The structure factor (1.55) in momentum space is given by

$$\Gamma_{\omega}(\mathbf{q}) \quad = \quad \gamma_e + \frac{\gamma_e}{\Omega}\sum_k \Gamma_{\omega}(\mathbf{q})\,\overline{G}^R_{\omega_0}(\mathbf{k})\,\overline{G}^A_{\omega_0-\omega}(\mathbf{k}-\mathbf{q}). \tag{1.67}$$

This expression can be factored into the form

$$\Gamma_\omega(\mathbf{q}) = \frac{\gamma_e}{1-\frac{p_0(\mathbf{q},\omega)}{\tau_e}}. \tag{1.68}$$

The Diffuson probability in momentum space is

$$\begin{aligned} p_d(\mathbf{q},\omega) &= \frac{c}{4\pi} p_0(\mathbf{q},\omega)^2 \Gamma_\omega(\mathbf{q}) \\ &= p_0(\mathbf{q},\omega) \frac{\frac{p_0(\mathbf{q},\omega)}{\tau_e}}{1-\frac{p_0(\mathbf{q},\omega)}{\tau_e}}. \end{aligned} \tag{1.69}$$

Using the approximation (1.66) the last expression rewrites as

$$p_d(\mathbf{q},\omega) = \frac{1}{-i\omega + Dq^2}. \tag{1.70}$$

We can use this result to verify that the Drude-Boltzmann term and the Diffuson give together a normalized probability. In the limit of weak scattering we have from (1.66)

$$\begin{aligned} p(\mathbf{q}=0,\omega) &= p_d + p_0 \\ &= p_0\left(1+\frac{\frac{p_0}{\tau_e}}{1-\frac{p_0}{\tau_e}}\right) \\ &= -\frac{i}{\omega}(1+i\omega\tau_e) \\ &= -\frac{i}{\omega} \end{aligned} \tag{1.71}$$

where in the last equality we neglected all terms of order $\mathscr{O}(\omega\tau)$.

1.6.2 The Cooperon

Taking the Fourier transform with respect to variable $\mathbf{r}-\mathbf{r}'$ of (1.60) we have

$$X_c(\mathbf{q},\omega) = \frac{2\pi\rho_0}{\Omega^2} \sum_{\mathbf{k},\mathbf{k}'} \overline{G}^R\left(\mathbf{k}+\frac{\mathbf{q}}{2}\right) \overline{G}^A\left(\mathbf{k}-\frac{\mathbf{q}}{2}\right) \Gamma'_\omega(\mathbf{k}+\mathbf{k}') \overline{G}^R\left(\mathbf{k}'+\frac{\mathbf{q}}{2}\right) \overline{G}^A\left(\mathbf{k}'-\frac{\mathbf{q}}{2}\right) \tag{1.72}$$

As was shown before, the Cooperon and Diffuson structure factors are identical, so that

$$\Gamma'_\omega(\mathbf{Q}) = \frac{\gamma_e}{1-\frac{p_0(\mathbf{Q},\omega)}{\tau_e}} \tag{1.73}$$

$$= \frac{\gamma_e}{\tau_e} \frac{1}{-i\omega + DQ^2} \tag{1.74}$$

$$= \frac{\gamma_e}{-i\omega\tau_e + \frac{1}{3}l_e^2 Q^2} \tag{1.75}$$

where $\mathbf{Q}=\mathbf{k}+\mathbf{k}'$ and in the second equality we used (1.66). We see that the structure factor has a peak about $\mathbf{Q}=0$ whose width[9] is $\frac{1}{kl_e}$. For the Cooperon therefore, the main contributions comes when $\mathbf{k}\approx-\mathbf{k}'$, and neglecting the dependence on $\mathbf{q}\ll\mathbf{k}$, we find by transforming (1.61)

$$\begin{aligned} X_c(\mathbf{q},\omega) &= \frac{1}{2\pi\rho_0\Omega^2}\sum_{\mathbf{k}}\left(\overline{G}^R(\mathbf{k})\,\overline{G}^A(\mathbf{k})\right)^2\sum_{\mathbf{Q}}\Gamma'_\omega(\mathbf{Q}) \\ &= \frac{\tau_e}{\pi\rho_0\Omega}\sum_{\mathbf{Q}}\frac{1}{-i\omega+DQ^2}. \end{aligned} \tag{1.76}$$

An important point is that the Cooperon contribution in this approximation has no dependence on $\mathbf{q}$. This is the result of the spatially localized nature of the Cooperon which is evident from the fact that (1.76) is proportional to the Fourier transform of $\Gamma'_\omega(\mathbf{r},\mathbf{r}')\,\delta(\mathbf{r}-\mathbf{r}')$.

1.7 Additional crossed diagrams

We noticed earlier (see (1.71)) that the Drude-Boltzmann term and the Diffuson give together a normalized probability. The inclusion of the Cooperon seems to violate this normalization. Looking at (1.64) we see the Cooperon contribution to the probability is positive for all scattering angles. This contribution should be compensated in order to restore the normalization of the probability. We address the issue of the existence of other possible contributions to the probability, which cancel out with the Cooperon. Indeed, there are two such contributions, of the same order of magnitude as the Cooperon which we must include. These two contributions $H^{(B)}$ and $H^{(C)}$ along with the Cooperon, which we designate also as $H^{(A)}$ to emphasize the relation between the three contributions, are known as Hikami boxes [13]. To see the motivation for such diagrams consider diagram (a) in figure (1.8) where the Cooperon structure factor is represented by the two vertical lines. Inserting a scattering event on one of the legs representing $\overline{G}^R_{1,2}$ changes nothing as such corrections are already included in the average Green's function (see section (1.2)). The lowest order possible correction in displayed in diagram (b). These diagrams corresponds to the second order Born approximation [10], where the propagating amplitudes can scatter up to two times from the same scatterer.

It is possible to insert additional scattering events in the path of the advanced or retarded waves as displayed in diagram (c), giving higher order contribution to the scattered amplitude. Each such impurity will add a factor

$$\gamma_e\int d\mathbf{r}'\overline{G}^R(\mathbf{r},\mathbf{r}')\,\overline{G}^R(\mathbf{r},\mathbf{r}') \tag{1.77}$$

for the retarded wave or

$$\gamma_e\int d\mathbf{r}'\overline{G}^A(\mathbf{r}',\mathbf{r})\,\overline{G}^A(\mathbf{r}',\mathbf{r}) \tag{1.78}$$

for the advanced wave.

Each of these terms contributes a factor of $\frac{1}{k_0 l_e}$ to the scattering amplitude compared to $H^{(A,B,C)}$.

[9] $Q\approx k\theta$ when $\theta\ll 1$ where θ is the angle between $\mathbf{k}$ and $\mathbf{k}'$

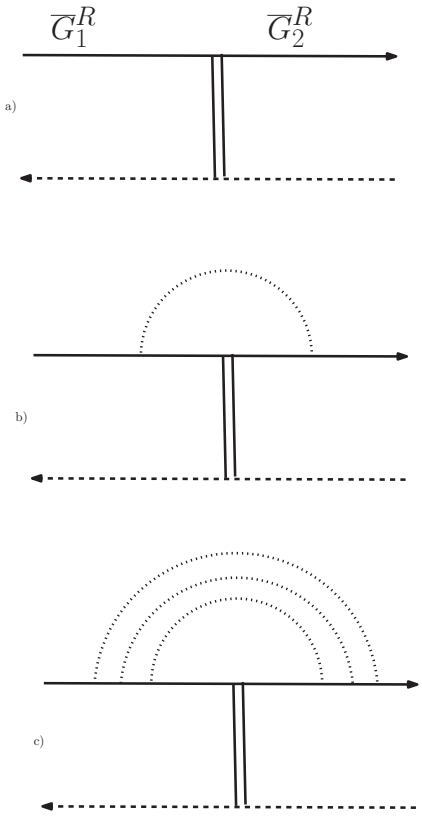

Figure 1.8: a) The Cooperon diagram. The structure factor is represented by the two vertical lines. b) One of the two leading diagrams in the second order Born approximation (in the other diagram the advanced amplitude, shown as a dashed line, goes through an additional scattering event). c) Higher order term. The contribution to the scattering amplitude of this diagram is reduced by a factor of $\frac{1}{(k_0 l_e)^2}$ with respect to the diagrams above it.

To construct these diagrams we start with the combination of Green's functions in the Cooperon[10]

$$H^{(A)}(\mathbf{r}_1,\mathbf{r}_2,\mathbf{r}_3,\mathbf{r}_4) = \overline{G}^R(\mathbf{r}_1,\mathbf{r}_2)\overline{G}^A(\mathbf{r}_4,\mathbf{r}_1)\overline{G}^R(\mathbf{r}_4,\mathbf{r}_3)\overline{G}^A(\mathbf{r}_3,\mathbf{r}_2) \tag{1.79}$$

Now insert an additional scattering event in the path of the retarded Green's function which will add the term $\gamma_e\delta(\mathbf{r}-\mathbf{r}')$

$$\begin{aligned} H^{(B)}(\mathbf{r}_1,\mathbf{r}_2,\mathbf{r}_3,\mathbf{r}_4) &= \gamma_e\int d\mathbf{r}'\overline{G}^R(\mathbf{r}_1,\mathbf{r}')\overline{G}^A(\mathbf{r}_4,\mathbf{r}_1)\overline{G}^R(\mathbf{r}',\mathbf{r}_2) \\ &\quad\times\overline{G}^R(\mathbf{r}',\mathbf{r}_3)\overline{G}^A(\mathbf{r}_3,\mathbf{r}_2)\overline{G}^R(\mathbf{r}_4,\mathbf{r}'). \end{aligned} \tag{1.80}$$

[10]These four Green's functions represent the two incoming and two outgoing amplitudes

By inserting the additional scattering event in the path of the second amplitude we construct $H^{(C)}$

$$\begin{aligned} H^{(C)}(\mathbf{r}_1,\mathbf{r}_2,\mathbf{r}_3,\mathbf{r}_4) &= \gamma_e \int \mathrm{d}\mathbf{r}' \overline{G}^R(\mathbf{r}_1,\mathbf{r}_2)\overline{G}^A(\mathbf{r}_3,\mathbf{r}')\overline{G}^R(\mathbf{r}_4,\mathbf{r}_3) \\ &\quad \times \overline{G}^A(\mathbf{r}_4,\mathbf{r}')\overline{G}^A(\mathbf{r}',\mathbf{r}_1)\overline{G}^A(\mathbf{r}',\mathbf{r}_2). \end{aligned} \tag{1.81}$$

The two additional Hikami boxes are depicted in figure (1.9). The combination of all three Hikami boxes (see figure 1.9) results in what is known as a dressed Cooperon

$$H = H^{(A)} + H^{(B)} + H^{(C)}. \tag{1.82}$$

The points $\mathbf{r}_2$ and $\mathbf{r}_4$ are the end points of the structure factor which we integrate over

$$H(\mathbf{r}_1 - \mathbf{r}_3) = \int d\mathbf{r}_2 d\mathbf{r}_4 H(\mathbf{r}_1,\mathbf{r}_2,\mathbf{r}_3,\mathbf{r}_4) \tag{1.83}$$

where the left hand side results from the translational invariance. The most important property of the dressed Cooperon is that its total contribution is zero

$$H = \int d\mathbf{R} H(\mathbf{R}) = 0. \tag{1.84}$$

To show this we define first the general function $f^{m,n}(\mathbf{R})$

$$f^{m,n}(\mathbf{R}') = \gamma_e \int \prod_{i=1}^{m} d\mathbf{r}_i \prod_{j=1}^{n} d\mathbf{r}'_j \overline{G}^R(\mathbf{r},\mathbf{r}_1)\ldots\overline{G}^R(\mathbf{r}_{m-1},\mathbf{r}_m)\overline{G}^A(\mathbf{r}_m,\mathbf{r}'_1)\ldots\overline{G}^A(\mathbf{r}'_n,\mathbf{r}') \tag{1.85}$$

with $\mathbf{R}' = |\mathbf{r} - \mathbf{r}'|$. In momentum space $f^{m,n}(\mathbf{R}=0)$ is given by

$$f^{m,n}(0) = \frac{\gamma_e}{\Omega}\sum_{\mathbf{k}} \left[\overline{G}^R(\mathbf{k})\right]^m \left[\overline{G}^A(\mathbf{k})\right]^n. \tag{1.86}$$

This reflects the fact that $f^{m,n}(\mathbf{R}'=0)$ is independent of the order of the sequence of the retarded and advanced Green's function. The function's value at $\mathbf{R}'=0$ is given by[8]

$$f^{m,n}(0) = i^{n-m}\frac{(n+m-2)!}{(n-1)!\,(m-1)!}\left(\frac{l_e}{2k_e}\right)^{n+m-2}. \tag{1.87}$$

Particularly we are interested in $f^{2,2}(0) = 2\left(\frac{l_e}{2k_e}\right)^2$ and $f^{2,1}(0) = \frac{il_e}{2k_e}$. The expression for the Cooperon, using the $f^{m,n}(\mathbf{R}')$ function as defined above, is given by

$$H^{(A)}(\mathbf{r_1} - \mathbf{r_3}) = \frac{1}{\gamma_e} f^{2,2}(0). \tag{1.88}$$

To see this we write $\frac{1}{\gamma_e} f^{2,2}(0)$ explicitly

$$\begin{aligned} \frac{1}{\gamma_e} f^{2,2}(0) &= \int \prod_{i=1}^{2} d\mathbf{r}_i \prod_{j=1}^{2} d\mathbf{r}'_j \delta(\mathbf{r}-\mathbf{r}')\overline{G}^R(\mathbf{r},\mathbf{r}_1)\ldots\overline{G}^R(\mathbf{r}_1,\mathbf{r}_2)\overline{G}^A(\mathbf{r}_2,\mathbf{r}'_1)\ldots\overline{G}^A(\mathbf{r}'_2,\mathbf{r}') \\ &= \int d\mathbf{r}_1 d\mathbf{r}_2 d\mathbf{r}'_1 d\mathbf{r}'_2 \overline{G}^R(\mathbf{r},\mathbf{r}_1)\overline{G}^R(\mathbf{r}_1,\mathbf{r}_2)\overline{G}^A(\mathbf{r}_2,\mathbf{r}'_1)\overline{G}^A(\mathbf{r}'_2,\mathbf{r}) \\ &= \int H^{(A)}(\mathbf{R})\, d\mathbf{R}. \end{aligned}$$

The two other contributions are given by

$$H^{(B,C)}(\mathbf{r_1}-\mathbf{r_3}) = \frac{1}{\gamma_e}\left[f^{2,1}(0)\right]^2. \tag{1.89}$$

When written explicitly we have

$$\begin{aligned}\frac{1}{\gamma_e}\left[f^{2,1}(0)\right]^2 &= \int d\mathbf{r_1}d\mathbf{r}d\mathbf{r}_4d\mathbf{r}'\gamma_e\delta(\mathbf{r}-\mathbf{r}')\overline{G}^R(\mathbf{r}_1,\mathbf{r})\overline{G}^R(\mathbf{r}_4,\mathbf{r}')\overline{G}^A(\mathbf{r}_4,\mathbf{r}_1)\\ &\quad\times\int d\mathbf{r}_2d\mathbf{r}_3d\mathbf{r}d\mathbf{r}'\overline{G}^R(\mathbf{r},\mathbf{r}_2)\overline{G}^A(\mathbf{r}_3,\mathbf{r}_2)\overline{G}^R(\mathbf{r}',\mathbf{r}_3)\\ &= \int d\mathbf{r}_1d\mathbf{r}_4d\mathbf{r}\gamma_e\overline{G}^R(\mathbf{r}_1,\mathbf{r})\overline{G}^R(\mathbf{r}_4,\mathbf{r})\overline{G}^A(\mathbf{r}_4,\mathbf{r}_1)\\ &\quad\times d\mathbf{r}_2d\mathbf{r}_3\overline{G}^R(\mathbf{r},\mathbf{r}_2)\overline{G}^A(\mathbf{r}_3,\mathbf{r}_2)\overline{G}^R(\mathbf{r},\mathbf{r}_3)\\ &= \int H^{(B)}(\mathbf{R})d\mathbf{R}\end{aligned}$$

We can see we have

$$\frac{2}{\gamma_e}\left[f^{2,1}(0)\right]^2+\frac{1}{\gamma_e}f^{2,2}(0)=\int d\mathbf{R}H(\mathbf{R})=0 \tag{1.90}$$

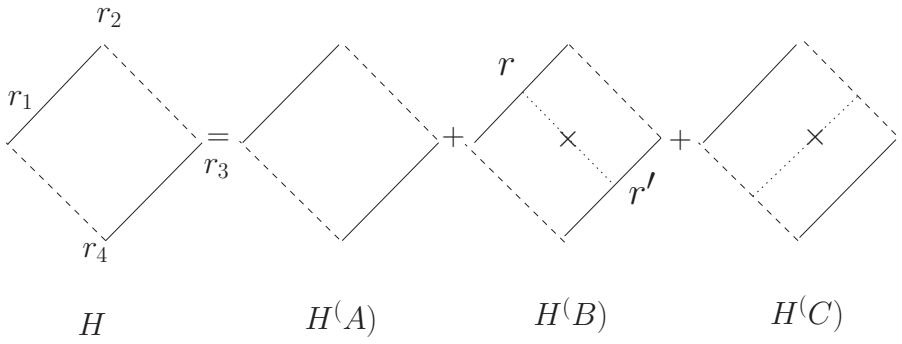

Figure 1.9: The dressed Cooperon is the sum of three Hikami boxes. These diagrams corresponds to the incoming and outgoing Green's function, omitting the structure factor.

Finally, one can construct additional diagrams which will contribute to the classical probability P_d by inserting more Cooperons and Diffusons in an alternating order [8]. This is very similar to way we treated the self energy Σ, where the Diffuson plays the role of the free propagator and the Cooperon the role of the scattering diagram in figure (1.3). This contribution is presented in figure (1.10) and leads to the following expression

$$P'_d(\mathbf{q},\omega) = P'_d(\mathbf{q},\omega)+P^2_d(\mathbf{q},\omega)\frac{I_c(\mathbf{q},\omega)}{\tau_e^2}+P^3_d(\mathbf{q},\omega)\left(\frac{I_c(\mathbf{q},\omega)}{\tau_e^2}\right)^2+\ldots \tag{1.91}$$

Figure 1.10: The sum of these diagrams contributes to the renormalization of the diffusion coefficient [8].

where $I_c(\mathbf{q},\omega) = Dq^2\tau_e X_c(\mathbf{q},\omega)$ is the contribution of the dressed Cooperon[11]. The term

$$P_d(\mathbf{q},\omega)\frac{I_c(\mathbf{q},\omega)}{\tau_e^2} = \frac{2\pi c^2}{3}\frac{l_e^3}{\Omega}\frac{q^2}{k_0^2 l_e^2}P_d(\mathbf{q},\omega)\sum_Q \frac{1}{-i\omega + DQ^2} \tag{1.92}$$

in the limit $k_0 l_e \gg 1$ which we work in is small, and the sum of the series is

$$P_d'(\mathbf{q},\omega) = \frac{P_d^2(\mathbf{q},\omega)}{1 - P_d(\mathbf{q},\omega)\frac{I_c(\mathbf{q},\omega)}{\tau_e^2}}. \tag{1.93}$$

This expression can be written in a form similar to that of the classical probability P_d by defining a renormalized diffusion coefficient D'

$$D' = D\left(1 - \frac{X_c(\mathbf{q},\omega)}{\tau_e}\right) \tag{1.94}$$

and

$$P_d'(\mathbf{q},\omega) = \frac{1}{-i\omega + D'q^2} \tag{1.95}$$

We see that the result of including the Cooperon contribution in the classical probability leads to a smaller diffusion coefficient, a phenomenon known as weak localization which appears also in conduction in disordered media.

[11] Notice that in the limit of week scattering $q \to 0$ it indeed vanishes.

Chapter 2

Coherent backscattering

In this section we examine the scattering of a monochromatic wave by a random medium. The bulk of the medium is considered large enough so our problem becomes scattering from a semi-infinite diffusive medium. We assume a plane wave, which hits the interface of the medium. Detectors are set up to measure the intensity scattered at different angles from the interface. The total incoming flux, the integral of the intensity across the beam cross section per unit time is

$$F_0 = I_0 S c \tag{2.1}$$

where c is the speed of light (which is the group velocity for a monochromatic wave), $I_0 \propto |E|^2$ the intensity which is proportional to the square of the electromagnetic field , and S the medium cross section. The scattered wave is spherical far enough from the source, and the measured flux per unit time and solid angle is

$$\frac{dF}{d\Omega} = cR^2 I(R\hat{s}_e) \tag{2.2}$$

where R is the distance to the detector and $I(R\hat{s}_e)$ is the angle dependent intensity which is measured by the detector located at a distance R from the medium. We are interested in the ratio between the scattered and the incoming fluxes, also called the albedo[1]

$$\alpha(\hat{s}_e) = \frac{1}{F_0}\frac{dF}{d\Omega} = \frac{R^2}{S}\frac{I(R\hat{s}_e)}{I_0} \tag{2.3}$$

For a random medium the two main contributions are the Diffuson and the Cooperon discussed in the previous chapter. Known as the incoherent and coherent albedo, respectively, they are two contributions which survive the averaging over the disorder. Each of them is composed of an incoming plane wave, a diffusion process inside the bulk and an outgoing spherical wave - the only difference is the time reversal of one the trajectories.

[1] The albedo depends on the inverse square of R as will be shown later, which cancels the dependence on R in (2.3).

2.1 Incoherent albedo

We consider a semi-infinite geometry with an interface at $z=0$, with $\mu(\mathbf{r})=0$ for $z<0$. For such a geometry[2] we expect all the incoming flux through $z=0$ to leave through the same interface[3]. A scalar wave propagates from the free medium in a direction $\hat{k}_i$ toward the interface at $z=0$ and crosses it at the point $\mathbf{r}$ as can be seen in figure 2.1. The incoming wave is

$$\psi_i(\mathbf{r}_1) = \sqrt{I_0}e^{-\frac{(\mathbf{r}_1-\mathbf{r})\cdot\hat{z}}{2l_e}}e^{i\mathbf{k}_i\cdot\mathbf{r}_1} \tag{2.4}$$

where the decaying exponential is the probability for free propagation until the first scattering event at $\mathbf{r}_1$. The contribution of the Diffuson to the intensity scattered in the direction $\hat{s}_e$ is given by

$$I_d(R\hat{s}_e) = \int d\mathbf{r}_1 d\mathbf{r}_2 \left|\psi(\mathbf{r}_1)\right|^2 \Gamma(\mathbf{r}_1,\mathbf{r}_2)\left|\overline{G}^R(\mathbf{r}_2,R)\right|^2 \tag{2.5}$$

where the Green's function represent the outgoing spherical wave, and R is the distance to the detector. Now, since the detector is located far apart from the interface, $\mathbf{R}$ is much greater than $\mathbf{r}_2$ which is of order of the elastic mean free path and we can use the Fraunhoffer approximation

$$|\mathbf{R}-\mathbf{r}_2| = |\mathbf{r}|\sqrt{1+\left(\frac{\mathbf{R}}{\mathbf{r}_2}\right)^2-2\frac{\mathbf{r}_2\cdot\mathbf{R}}{|\mathbf{r}_2|^2}} \approx |\mathbf{r}_2|-\frac{\mathbf{r}_2\cdot\mathbf{R}}{|\mathbf{r}_2|} \tag{2.6}$$

for the above mentioned Green's function

$$\overline{G}^R(\mathbf{r}_2,R) \approx e^{-\frac{(\mathbf{r}'-\mathbf{r}_2)\cdot\hat{z}}{2l_e}}e^{-i\mathbf{k}_0\cdot\mathbf{r}_2}\frac{e^{ik_0R}}{4\pi R}. \tag{2.7}$$

Using the explicit form (2.4) we can write (2.5) as follows

$$I_d(R\hat{s}_e) = \frac{I_0}{(4\pi)^2R^2}\int d\mathbf{r}_1 d\mathbf{r}_2 e^{-\frac{(\mathbf{r}_1-\mathbf{r})\cdot\hat{z}}{l_e}}\Gamma(\mathbf{r}_1,\mathbf{r}_2)e^{-\frac{(\mathbf{r}'-\mathbf{r}_2)\cdot\hat{z}}{l_e}}. \tag{2.8}$$

For a normal incoming wave we can replace $|\mathbf{r}_1-\mathbf{r}|=z_1$ and $|\mathbf{r}_2-\mathbf{r}'|=\frac{z_2}{\mu}$, with $\mu=\cos\theta$, the cosine of the angle between the normal to the interface and the outgoing wave (see figure (2.1))

$$I_d(R,\mu) = \frac{I_0}{(4\pi)^2R^2}\int d\mathbf{r}_1 d\mathbf{r}_2 e^{-\frac{\mathbf{z}_1-\mathbf{z}}{l_e}}\Gamma(\mathbf{r}_1,\mathbf{r}_2)e^{-\frac{\mathbf{z}'-\mathbf{z}_2}{\mu l_e}} \tag{2.9}$$

It was shown in the previous chapter that in the weak disorder limit the structure factor is a solution of a classical diffusion equation (1.56) and is related to $p_d(\mathbf{r}_1,\mathbf{r}_2)$ through

$$p_d(\mathbf{r}_1,\mathbf{r}_2) = \frac{l_e^2}{4\pi c}\Gamma(\mathbf{r}_1,\mathbf{r}_2). \tag{2.10}$$

The Diffuson contribution to the intensity is then

$$I_d = \frac{I_0 c}{4\pi l_e^2}\frac{S}{R^2}\int_0^\infty\int_0^\infty dz_1 dz_2 e^{-\frac{z_1}{l_e}}p_d(z_1,z_2)e^{-\frac{z_2}{\mu l_e}} \tag{2.11}$$

[2] The origin can be taken at any point in the plane $z=0$ due to translational symmetry in the $\hat{x},\hat{y}$ directions.

[3] Under the assumption of elastic scatterings.

where $p_d(z_1,z_2) = \int_S d^2\rho\, p_d(\rho,z_1,z_2)$ is the diffusion probability for a semi-infinite medium, and ρ is the projection of the vector $\mathbf{r}_1 - \mathbf{r}_2$ on the plane $z = 0$. Using the image method [8] we calculate

$$p_d(\rho,z_1,z_2) = \frac{1}{4\pi D}\left[\frac{1}{\sqrt{\rho^2+(z_1-z_2)^2}} - \frac{1}{\sqrt{\rho^2-(z_1+z_2+2z_0)^2}}\right] \tag{2.12}$$

with[4] $z_0 = \frac{2l_e}{3}$. Integrating over ρ we get

$$\begin{aligned} p_d(z_1,z_2) &= \frac{1}{2D}\left[z_1+z_2+2z_0-|z_1-z_2|\right] \\ &= \frac{z_m+z_0}{2D} \end{aligned}$$

with $z_m = \min(z_1,z_2)$. Integrating over the z coordinate we find the incoherent albedo to be

$$\alpha_d = \frac{3}{4\pi}\mu\left(\frac{z_0}{l_e}+\frac{\mu}{\mu+1}\right). \tag{2.13}$$

2.2 Coherent albedo

The calculation of the Cooperon contribution (see figure 2.1) to the albedo is obtained in a similar way to the Diffuson. The contribution of the Cooperon to the scattered intensity is

$$I_c(R\hat{s}_e) = I_0\int d\mathbf{r_1}d\mathbf{r}_2\psi(\mathbf{r}_1)\,\psi^*(\mathbf{r}_2)\,\Gamma(\mathbf{r}_1,\mathbf{r}_2)\,\overline{G}^R(\mathbf{r}_2,R)\,\overline{G}^A(R,\mathbf{r}_1) \tag{2.14}$$

We use the Fraunhoffer approximation again, and for an incoming plane wave normal to the interface

$$I_c(R\hat{s}_e) = I_0\frac{1}{(4\pi R)^2}\int d\mathbf{r_1}d\mathbf{r}_2 e^{-\frac{z_1}{2l_e}}e^{ik_i\cdot z_1}e^{-\frac{z_2}{2l_e}}e^{-ik_i\cdot z_2}\Gamma'(\mathbf{r}_1,\mathbf{r}_2)\,e^{-\frac{z_2}{2l_e\mu}}e^{-i\mathbf{k}_e\cdot\mathbf{r}_2}e^{-\frac{z_1}{2l_e\mu}}e^{i\mathbf{k}_e\cdot\mathbf{r}_1}.$$

Collecting the terms together we find the coherent albedo to be

$$\alpha_c = \frac{1}{(4\pi)^2 S}\int d\mathbf{r}_1 d\mathbf{r}_2 e^{-\left(\frac{\mu+1}{2\mu}\right)\frac{z_1+z_2}{l_e}}\Gamma(r_1,r_2)\,e^{i\left(\hat{\mathbf{k}}_i+\hat{\mathbf{k}}_e\right)\cdot(\mathbf{r}_1-\mathbf{r}_2)} \tag{2.15}$$

Here the phase difference between the two trajectories manifests itself in the complex exponential. We see that when the incoming and outgoing waves have opposite directions the phase term cancels. For $\mu = 1$ (the incoming and outgoing waves are parallel) we find

$$\begin{aligned} \alpha_c &= \frac{1}{(4\pi)^2 S}\int d\mathbf{r}_1 d\mathbf{r}_2 e^{-\frac{z_1+z_2}{l_e}}\Gamma(r_1,r_2) \\ &= \alpha_d(\mu=1) \end{aligned}$$

[4] For the geometry in this problem $p(z_1,z_2)$ is solution of the diffusion equation with the boundary condition that it vanishes for $z = -z_0$. See appendix A5.2.3 of [8].

Thus the back scattered intensity is enhanced by a factor 2 due to the Cooperon. The explicit expression for the coherent albedo after the integration is[5]

$$\alpha_c(k_\perp,\mu) = \frac{3}{8\pi}\frac{1}{\left(\frac{\mu+1}{2\mu}+|\mathbf{k}_\perp|l_e\right)^2}\left(\frac{2\mu}{\mu+1}+\frac{1-e^{-2|\mathbf{k}_\perp|z_0}}{|\mathbf{k}_\perp|l_e}\right) \tag{2.16}$$

with $\mathbf{k}_\perp = \left(\hat{\mathbf{k}}_i+\hat{\mathbf{k}}_e\right)_\perp$. To see why we neglect $(\mathbf{r}_1-\mathbf{r}_2)_z$, that is the projection of $\mathbf{r}_1-\mathbf{r}_2$ along the z direction, we turn to equation (2.15). The coherent albedo, α_c, is strongly attenuated in the z direction so only values of z_1 and z_2 which are small compared to l_e contribute. This means that $|z_1-z_2|$ will usually be much smaller than ρ which enters only through the structure factor, a quantity which we assume to vary slowly on a scale of l_e.

In the weak disorder limit, where $k_0 l_e \gg 1$, we see why the Cooperon contribution is limited to small angles. $\mathbf{k}_\perp \approx \mathbf{k}\sin(\theta)$ with a $k_0 l_e$ having a typical value of order of $\mathcal{O}\left(10^2\right)$. For example, when $\theta = 0.1$rad and $k_0 l_e = 100$ the albedo already decreases to 0.1% of its value for $\theta = 0$.

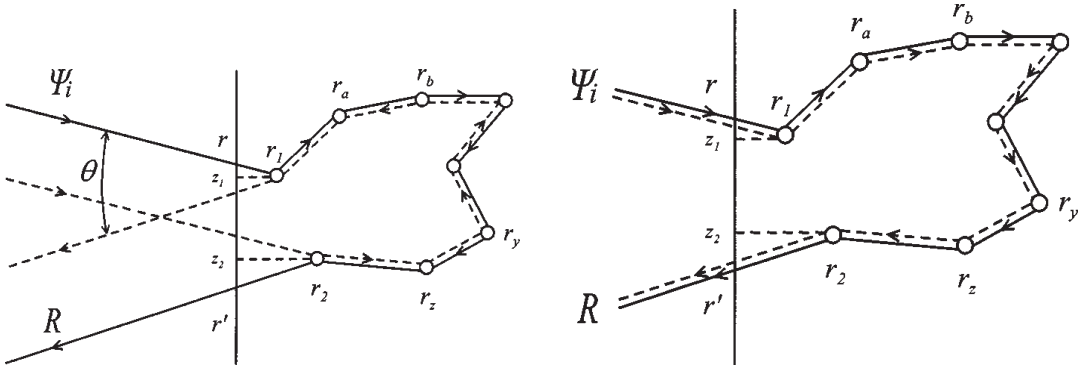

Figure 2.1: The contribution of the Diffuson (right) and Cooperon (left) to the albedo [8]

A typical experimental setup is described in appendix (C). The phenomenon of coherent back scattering was observed in many experiments. A good source for a list of selected reports is found in the references section of [8]. An example of an experimental validation of (2.13) and (2.16) is shown in figure (2.2). It is evident from the figure that the Cooperon contribution is indeed positive for all scattering angles. With the Diffuson and the Drude-Boltzman contribution being normalized, the Cooperon contribution seems to violate energy conservation. In the following chapters we demonstrate how this problem is resolved.

[5] A more detailed calculation of the Cooperon contribution to the albedo is found in [8].

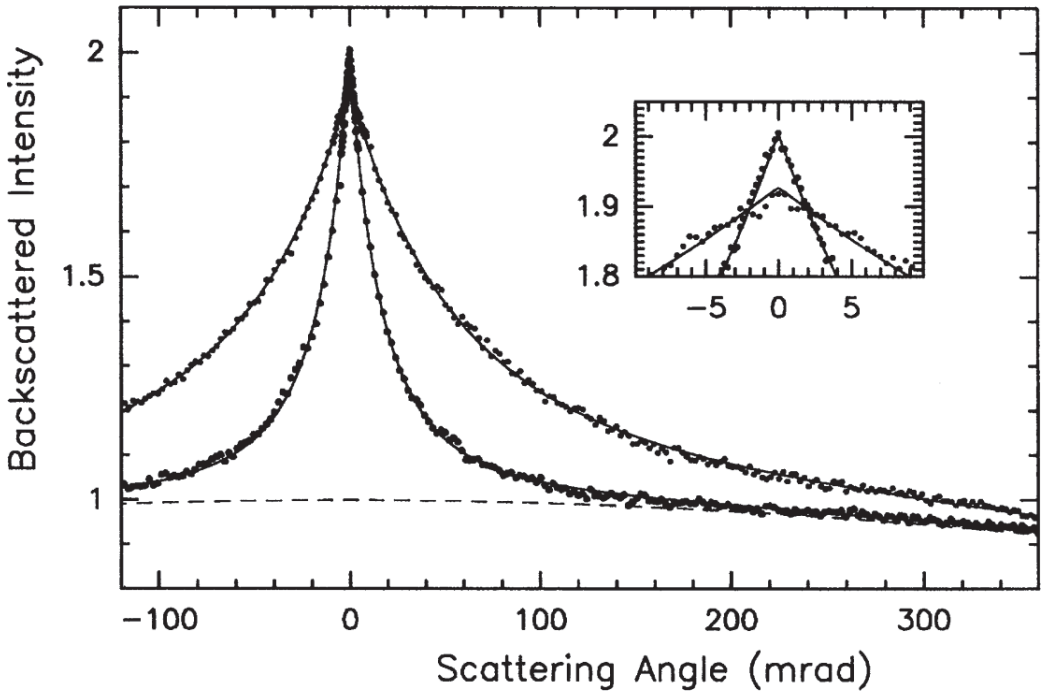

Figure 2.2: A plot of the backscattered intensity vs. angle. The solid line represent the Cooperon contribution (2.16) *while the dashed line represent the Diffuson contribution* (2.13) *[14]. The broad cone is for a* TiO_2 *sample with* $kl_e = 5.8 \pm 1$ *and the narrow cone is for a* $BaSO_4$ *sample with* $kl_e = 22.6 \pm 1$.

Chapter 3

Dephasing

In Chapter 1, two scattering processes which contribute to the scattered intensity, namely the Diffuson and Cooperon, were introduced. In that chapter we treated only the problem of scalar waves. We now wish to extend the theory to include polarization as well. To that end we first extend the description of the scattering events to include the polarization degrees of freedom.

In the limit where the wave length of the radiation is much larger than the size of the scatterers, also known as Rayleigh scattering, the polarization $\mathbf{P}'$ of the scattered wave depends on the incoming wave polarization $\hat{\mathbf{P}}$ and the scattered wave vector $\hat{\mathbf{k}}' = \left(\hat{k}_x, \hat{k}_y, \hat{k}_z\right)$

$$\hat{\mathbf{P}}' = -\hat{\mathbf{k}}' \times \left(\hat{\mathbf{k}}' \times \hat{\mathbf{P}}\right) \tag{3.1}$$

This can be written in matrix form

$$\mathbf{P}' = M\left(\hat{\mathbf{k}}'\right)\mathbf{P} \tag{3.2}$$

$$M\left(\hat{\mathbf{k}}\right) = \begin{pmatrix} 1-\hat{k}_x^2 & -\hat{k}_x\hat{k}_y & -\hat{k}_x\hat{k}_z \\ -\hat{k}_x\hat{k}_y & 1-\hat{k}_y^2 & -\hat{k}_y\hat{k}_z \\ -\hat{k}_x\hat{k}_z & -\hat{k}_y\hat{k}_z & 1-\hat{k}_z^2 \end{pmatrix} \tag{3.3}$$

We define the classical polarizability of the medium $\alpha = \frac{\upsilon\delta\varepsilon}{\varepsilon}$ where υ is the volume of the scatterer. The scattering amplitude is given by the following tensor

$$\nu_{\alpha\beta}\left(\hat{\mathbf{k}}'\right) = \nu_0 M\left(\hat{\mathbf{k}}\right) = \nu_0\left(\delta_{\alpha\beta} - \hat{k}'_\alpha\hat{k}'_\beta\right) \tag{3.4}$$

where $\nu_0 = \alpha_0 k_0^2$ replaces the scalar scattering potential of the Edwards model in (1.5), and the indices α, β take one of the Cartesian components x, y, z. The scattering amplitude is now related to the change in polarization as shown in figure (3.1). The correlation function of the scalar Gaussian model (1.6) is generalized to the following form

$$B_{\alpha\beta,\gamma\delta} = n_i \nu_{\alpha\gamma}\nu_{\beta\delta}. \tag{3.5}$$

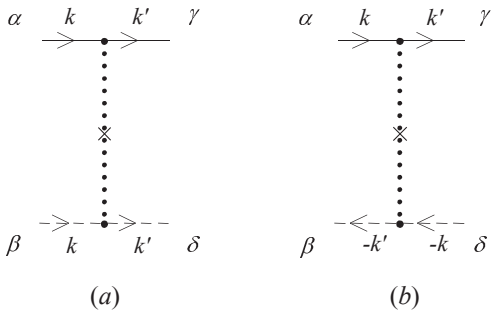

Figure 3.1: The interaction vertex for a polarized wave. Diagram (a) represents the interaction vertex of a Diffuson, and diagram (b) of a Cooperon.[8]

For a scalar wave we defined γ_e to be the average over the correlation function (1.2), where the averaging is over the directions of $\hat{\mathbf{k}}'$

$$\gamma_e = \left\langle B\left(\mathbf{k}-\mathbf{k}'\right)\right\rangle. \tag{3.6}$$

The introduction of polarization requires us to average not only over all possible scattering directions, but also over all possible polarizations of the outgoing wave

$$\gamma_{pol} = \sum_{\beta}\left\langle B_{\alpha\alpha,\beta\beta}\right\rangle. \tag{3.7}$$

Using (3.5) γ_{pol} for a wave with polarization in the α direction is

$$\gamma_{pol} = n_i v_0^2 \sum_{\beta}\left\langle M_{\alpha\beta}M_{\beta\alpha}\right\rangle = \frac{2}{3}\gamma_e. \tag{3.8}$$

From (1.38) we see that the elastic mean free path is also modified

$$l_{pol} = \frac{3}{2}l_e. \tag{3.9}$$

The longer mean free path l_{pol} is the result of the restriction imposed by (3.1) on the direction of the scattered wave. In (3.8) all polarization directions are averaged over equally. In the absence of equation (3.1) the scattering amplitude (3.8) would be independent of the polarization and $\gamma_{pol} = l_{pol}$. However, due to (3.1) the correlation function $B_{\alpha\beta,\gamma\delta}$ is proportional to the scattering cross section given by the Rayleigh formula

$$\sigma\left(\mathbf{k},\mathbf{k}',\hat{\mathbf{P}}\right) = \frac{k_0^4\alpha^2}{16\pi^2}\left(1-\left(\mathbf{k}'\cdot\hat{\mathbf{P}}\right)^2\right). \tag{3.10}$$

Therefore scattering is most likely when $\hat{\mathbf{P}}$ is normal to $\mathbf{k}'$, which also means $\hat{\mathbf{P}} = \hat{\mathbf{P}}'$. The scattering angles now are more inclined to be in a plane perpendicular to $\hat{\mathbf{P}}$. This restriction limits the possible scattering trajectories and forces a greater number of scatterings before leaving the medium. When considering the elastic mean free path, we can think of the polarized case as a scalar one with a longer elastic mean free path.

3.1 The structure factor

When polarization is taken into consideration the scattering depends on the four polarizations of the two incoming amplitudes (α,β) and the two outgoing ones (γ,δ). These states associate to the interaction vertex a tensor which couples between the incoming and outgoing polarizations [8]

$$b_{\alpha\beta,\gamma\delta}=\overline{M_{\alpha\beta}M_{\beta\alpha}}=\frac{1}{15}\left(6\delta_{\alpha\gamma}\delta_{\beta\delta}+\delta_{\alpha\delta}\delta_{\beta\gamma}+\delta_{\gamma\delta}\delta_{\alpha\beta}\right). \tag{3.11}$$

The tensor (3.11) can be cast into a 9×9 matrix form

$$\frac{1}{15}\begin{pmatrix} 8&0&0&0&1&0&0&0&1\\ 0&6&0&1&0&0&0&0&0\\ 0&0&6&0&0&0&1&0&0\\ 0&1&0&6&0&0&0&0&0\\ 1&0&0&0&8&0&0&0&1\\ 0&0&0&0&0&6&0&1&0\\ 0&0&1&0&0&0&6&0&0\\ 0&0&0&0&0&1&0&6&0\\ 1&0&0&0&1&0&0&0&8 \end{pmatrix} \tag{3.12}$$

The elements with the largest values are on the main diagonal, indicating that the polarization is more likely not to change after a scattering event. Inserting $b_{\alpha\beta,\gamma\delta}$ into (1.67) (where for a scalar wave $b_{\alpha\beta,\gamma\delta}=1$) we have the following iterative equation (compare with (1.67))

$$\Gamma_{\alpha\beta,\gamma\delta}(\mathbf{q})=\gamma_e b_{\alpha\beta,\gamma\delta}+\sum_{\mu,\nu}\Gamma_{\alpha\beta,\mu\nu}(\mathbf{q})\,b_{\mu\nu,\gamma\delta}w(\mathbf{q}). \tag{3.13}$$

The function $w(\mathbf{q})=\frac{3}{2}\left(1-Dq^2\tau_{pol}\right)$ with $\tau_{pol}=\frac{3}{2}\tau_e$ comes from the Drude-Boltzmann approximation in momentum space[1], and the diffusion constant is $D=\frac{1}{3}c^2\tau_{pol}=\frac{1}{3}cl_{pol}$. The presence of l_{pol} and τ_{pol} in $w(q)$ which was defined for the scalar problem comes from the modification of the elastic mean free time and length due to the polarization. The matrix (3.12) can be diagonalized, giving three[2] eigenvalues denoted by $k=0,1,2$.

$$\begin{aligned} b_{(k=0)} &= \frac{2}{3}\\ b_{(k=1)} &= \frac{1}{3}\\ b_{(k=2)} &= \frac{7}{15}. \end{aligned} \tag{3.14}$$

In the diagonal basis (3.11) is now

$$b_{\alpha\beta,\gamma\delta}=\frac{1}{2}(b_1+b_2)\,\delta_{\alpha\gamma}\delta_{\beta\delta}+\frac{1}{2}(-b_1+b_2)\,\delta_{\alpha\delta}\delta_{\beta\gamma}+\frac{1}{2}(b_0-b_2)\,\delta_{\alpha\beta}\delta_{\gamma\delta}. \tag{3.15}$$

[1] See (1.66) and (1.65)

[2] $b_{(k=1)}$ and $b_{(k=2)}$ have a degeneracy of 3 and 5 respectively.

This tensor is a product of two rank-2 tensors in a three-dimensional space and therefore can be decomposed into the sum of three irreducible tensors: a scalar, an antisymmetric and traceless symmetric.

$$\begin{aligned} T^{(0)}_{\alpha\beta,\gamma\delta} &= \frac{1}{3}\delta_{\alpha\beta}\delta_{\gamma\delta} \\ T^{(1)}_{\alpha\beta,\gamma\delta} &= \frac{1}{2}\left[\delta_{\alpha\gamma}\delta_{\beta\delta} - \delta_{\alpha\delta}\delta_{\beta\gamma}\right] \\ T^{(2)}_{\alpha\beta,\gamma\delta} &= \frac{1}{2}\left[\delta_{\alpha\gamma}\delta_{\beta\delta} + \delta_{\alpha\delta}\delta_{\beta\gamma}\right] - \frac{1}{3}\delta_{\alpha\beta}\delta_{\gamma\delta}. \end{aligned} \tag{3.16}$$

These tensors are orthogonal

$$\sum_{\mu,\nu} T^{(k)}_{\alpha\beta,\mu\nu} T^{(k')}_{\mu\nu,\gamma\delta} = \delta_{kk'} T^{(k)}_{\alpha\beta,\gamma\delta} \tag{3.17}$$

and their sum is the unity

$$\sum_{k} T^{(k)}_{\alpha\beta,\gamma\delta} = 1. \tag{3.18}$$

These properties allow us to write the polarization tensor as their linear combination

$$b_{\alpha\beta,\gamma\delta} = \sum_{k=0}^{2} b_k T^{(k)}_{\alpha\beta,\gamma\delta}. \tag{3.19}$$

Since the subspaces are orthogonal we can treat (3.13) as a scalar equation in each subspace

$$\Gamma_k(\mathbf{q}) = \gamma_e b_k + \Gamma_k(\mathbf{q})\, b_k w(\mathbf{q}) \tag{3.20}$$

and solve it appropriately. We thus obtain three distinct modes

$$\Gamma_k = \frac{\gamma_e b_k}{1 - b_k w(q)} = \frac{\gamma_{pol}/\tau_{pol}}{\frac{1}{\tau_k} + Dq^2} \tag{3.21}$$

which are characterized by a relaxation time

$$\tau_k = \tau_{pol} \frac{b_k}{\frac{2}{3} - b_k}. \tag{3.22}$$

For the three distinct modes we have

$$\Gamma_0(q) = \frac{\gamma_{pol}/\tau_{pol}}{Dq^2} \tag{3.23}$$

$$\Gamma_1(q) = \frac{\gamma_{pol}/\tau_{pol}}{\frac{1}{\tau_{pol}} + Dq^2} \tag{3.24}$$

$$\Gamma_2(q) = \frac{\gamma_{pol}/\tau_{pol}}{\frac{3}{7\tau_{pol}} + Dq^2}. \tag{3.25}$$

Taking the Fourier transform with respect to the momentum $\mathbf{q}$ we see that the modes with[3] $k \neq 0$ have an exponential time decay with a characteristic time of the order τ_{pol}. (3.13) can now be written as

$$\Gamma_{\alpha\beta,\gamma\delta} = \sum_{k=0}^{2} \Gamma_k T^{(k)}_{\alpha\beta,\gamma\delta} = \Gamma_0 T^{(0)} + \Gamma_1 T^{(1)} + \Gamma_2 T^{(2)} \tag{3.26}$$

[3] k here is not a momentum but the index of the three irreducible tensors $T^{(k)}_{\alpha\beta,\gamma\delta}$.

which, by using (3.16), gives the following result

$$\Gamma_{\alpha\beta,\gamma\delta} = \frac{1}{2}(\Gamma_1+\Gamma_2)\,\delta_{\alpha\gamma}\delta_{\beta\delta} + \frac{1}{2}(-\Gamma_1+\Gamma_2)\,\delta_{\alpha\delta}\delta_{\beta\gamma} + \frac{1}{3}(\Gamma_0-\Gamma_2)\,\delta_{\alpha\beta}\delta_{\gamma\delta} \tag{3.27}$$

This last result allows us to calculate the contribution of the Diffuson and the Cooperon to the scattered intensity for a polarized wave. We consider the case of an incoming wave and its conjugate, having the same polarization (since they emerge from the same source). This means $\alpha=\beta$ for the Diffuson and $\alpha=\gamma$ for the Cooperon in (3.27). The outgoing amplitudes also have the same polarization ($\gamma=\delta$ and $\beta=\delta$ respectively). The contributions of the Diffuson and the Cooperon for a polarized wave are presented in table 3.1.

	Diffuson	Cooperon
Parallel ($\alpha=\delta$)	$\Gamma_{\alpha\alpha,\alpha\alpha}=\frac{1}{3}(\Gamma_0+2\Gamma_2)$	$\Gamma_{\alpha\alpha,\alpha\alpha}=\frac{1}{3}(\Gamma_0+2\Gamma_2)$
Perpendicular ($\alpha\neq\delta$)	$\Gamma_{\alpha\alpha,\beta\beta}=\frac{1}{3}(\Gamma_0-\Gamma_2)$	$\Gamma_{\alpha\beta,\beta\alpha}=\frac{\Gamma_2-\Gamma_1}{2}$

Table 3.1: Contribution of the Diffuson and Cooperon in different channels

From table (3.1) we learn that both the Diffuson and the Cooperon have their contribution to the parallel channel attenuated compared to their scalar value, although their relative magnitude remains the same. On the other hand, only the Diffuson contributes to the perpendicular channel, as the Cooperon contribution is proportional to the Γ_1 and Γ_2 modes which decay rapidly. Notice also that the Diffuson contributes equally in each polarization channel

$$\sum_{\beta}\Gamma_{\alpha\alpha,\beta\beta}=\Gamma_0 \tag{3.28}$$

This results from conservation of energy. That is, the sum of the contributions in all channels, which constitute the Diffuson for a polarized wave, is equal to the total contribution of the Diffuson for a scalar wave.

Chapter 4

Dephasing in $H^{(B)}$and $H^{(C)}$

It was demonstrated in section 1.7 that the contribution to the scattered intensity of all three Hikami boxes is zero. In the previous chapter we saw that the Cooperon contribution for a polarized light is different from scalar case. The scattered intensity in the parallel channel is decreased by two thirds, while in the perpendicular channel the scattered intensity is zero. This naturally raises the question if the contribution of the three Hikami boxes is still zero. We must therefore find how the two other Hikami boxes, which differ from the Cooperon due to the additional impurity, behave when polarization is considered. In (3.1) we diagonalized the interaction vertex in order to decouple the different modes. However, for $H^{(B,C)}$ it is more convenient to work with a different set of tensor projectors than (3.16), which allow us to couple the added impurity (see figure (4.1)) more conveniently to the crossed diagrams [15]. The new set of tensor projectors is created by exchanging the second and forth index in (3.16)

$$\mathscr{T}^{(0)}_{\alpha\delta,\gamma\beta} = \frac{1}{3}\delta_{\alpha\delta}\delta_{\gamma\beta} \tag{4.1}$$

$$\mathscr{T}^{(1)}_{\alpha\delta,\gamma\beta} = \frac{1}{2}\left(\delta_{\alpha\gamma}\delta_{\beta\delta} - \delta_{\alpha\beta}\delta_{\delta\gamma}\right) \tag{4.2}$$

$$\mathscr{T}^{(2)}_{\alpha\delta,\gamma\beta} = \frac{1}{2}\left(\delta_{\alpha\gamma}\delta_{\beta\delta} + \delta_{\alpha\beta}\delta_{\delta\gamma}\right) - \frac{1}{3}\delta_{\alpha\delta}\delta_{\gamma\beta}. \tag{4.3}$$

The former set of projectors (3.16) can be expressed in terms of the new ones

$$\begin{aligned} T^{(0)} &= \frac{1}{3}\left(\mathscr{T}^{(2)} - \mathscr{T}^{(1)} + \mathscr{T}^{(0)}\right) \\ T^{(1)} &= \frac{1}{2}\left(\mathscr{T}^{(2)} + \mathscr{T}^{(1)} - 2\mathscr{T}^{(0)}\right) \\ T^{(2)} &= \frac{5}{3}\mathscr{T}^{(0)} + \frac{5}{6}\mathscr{T}^{(1)} + \frac{1}{6}\mathscr{T}^{(2)} \end{aligned} \tag{4.4}$$

and the structure factor in the new basis is

$$\begin{aligned} \Gamma_{\alpha\beta,\gamma\delta} = &\left(\frac{\Gamma_0}{3} - \Gamma_1 + \frac{5}{3}\Gamma_2\right)\mathscr{T}^{(0)} \\ &+ \left(-\frac{\Gamma_0}{3} + \frac{\Gamma_1}{2} + \frac{5}{6}\Gamma_2\right)\mathscr{T}^{(1)} + \left(\frac{\Gamma_0}{3} + \frac{\Gamma_1}{2} + \frac{\Gamma_2}{6}\right)\mathscr{T}^{(2)}. \end{aligned} \tag{4.5}$$

The two Hikami boxes contain an additional impurity which is described by the interaction (3.11). This interaction couples to the structure factor. Expressing the interaction as a superposition of the tensor projection, we can use the orthogonality of the projectors to treat the scattered intensity as a sum of scalar intensities. Since we know that only the scalar mode $\Gamma_{k=0}$ will contribute we need not calculate for the $k = 1,2$ modes.

4.1 The scalar mode

At the end of the previous chapter we saw that the scattering of a polarized wave can be separated into three distinct modes we designated as Γ_k. Of the three, the modes $k = 1,2$ were characterized by a quick time decay. This leaves the $k = 0$ mode which diverges for small frequencies and large wave length mode, as the only contributing mode in our approximation, which is valid for time scales much greater than the elastic mean free time. This is the same approximation we used to relate the structure factor to the solution of the diffusion equation in section 1.4. We generalize (1.79) and (1.80) to the polarized case employing the same procedure used in (3.1), that is by replacing the scalar scattering potential with (3.4) giving in momentum space [15]

$$H^{(B)}_{\alpha b,a\gamma}(\mathbf{q}) = b_{\alpha b,a\gamma}H^{(B)}(\mathbf{q}) \tag{4.6}$$

$$H^{(C)}_{\alpha\delta,\beta b}(\mathbf{q}) = b_{\beta b,a\delta}H^{(B)}(\mathbf{q}). \tag{4.7}$$

Using (3.16) and (3.19) it is easy to calculate that in the parallel channel

$$H^{(B)}_{\alpha\alpha,\alpha\alpha}(\mathbf{q}) = \frac{1}{5}H^{(B)}(\mathbf{q}) \tag{4.8}$$

$$H^{(C)}_{\alpha\alpha,\alpha\alpha}(\mathbf{q}) = \frac{1}{5}H^{(B)}(\mathbf{q}). \tag{4.9}$$

It seems that (1.84) is no longer valid. However, $H^{(B,C)}$ differ from $H^{(A)}$ in the way the extra impurity couples to the structure factor. In this section we calculate the effect of this coupling to see how it modifies the structure factor.

4.1.1 Parallel channel

Consider diagram (4.1) which represents $H^{(B)}$ and indicates the polarizations during free propagation.

The contribution to the $k = 0$ mode[1] is given by[15]

$$\begin{aligned} X^{(k=0)}_{\alpha\delta,\gamma\beta} &\propto \sum_{a,b,k'} b^{(k')}_{\alpha b,a\gamma}\Gamma^{(k=0)}_{a\beta,b\delta} \\ &= \sum_{a,b,k'} b^{(k')}\Gamma_0\mathscr{T}^{(k')}_{\alpha b,a\gamma}\mathscr{T}^{(k=0)}_{a\beta,b\delta}. \end{aligned} \tag{4.10}$$

[1] We only consider here the $\Gamma_{k=0}$, the zero mode of the structure factor which does not decay exponentially. We still need to sum over all three modes for the additional vertex b_k.

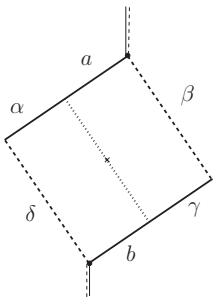

Figure 4.1: A schematic drawing of the polarization of the radiation for the Hikami box $H^{(B)}$. The two lines marked with α and δ represent the incoming amplitudes with their respected polarization. The lines marked with β and γ represent the outgoing amplitudes. The fine dashed line represent the scattering due to the additional impurity. a,b are the polarization directions which are summed over in (4.10)*.*

The Hikami boxes enter through $b^{(k')}_{\alpha b,a\gamma}$. By exchanging the places of the β and δ we have a and β as the polarizations going into the structure factor and b and δ as the outgoing ones. For the parallel case we have

$$X^{(k=0)}_{\alpha\alpha,\alpha\alpha} \propto \frac{\Gamma_0}{3} \sum_{a,b,k'} b^{(k')} \mathscr{T}^{(k')}_{\alpha b,a\alpha} \tag{4.11}$$

The tensor $\mathscr{T}^{(0)}_{a\alpha,b\alpha}$ implies that $a = b = \alpha$ (else it will be zero), which allows to write $\mathscr{T}^{(0)}_{a\alpha,b\alpha} = \frac{1}{3}$. The intimidate polarizations a,b take on the values x,y,z. Due to the isotropy of the medium each sum contributes the same as the other. This triple contribution cancels the $1/3$ factor leaving us with

$$X^{(k=0)}_{\alpha\alpha,\alpha\alpha} \quad \propto \quad \Gamma_0 \sum_{k'} b^{(k')} \mathscr{T}^{(k')}_{\alpha a,a\alpha}. \tag{4.12}$$

We calculate now for each k':

1. $k' = 0$

$$\begin{aligned} \mathscr{T}^{(k'=0)}_{\alpha a,a\alpha} &= \frac{1}{3}\delta_{\alpha a}\delta_{a\alpha} \\ &= \frac{1}{3}\delta_{aa} \\ &= \frac{1}{3} \end{aligned} \tag{4.13}$$

2. $k'=1$

$$\mathscr{T}^{(k'=1)}_{\alpha a,a\alpha} = \frac{1}{2}\left[\delta_{a\alpha}\delta_{a\alpha}-\delta_{\alpha\alpha}\delta_{aa}\right]=0 \tag{4.14}$$

3. $k'=2$

$$\begin{aligned}\mathscr{T}^{(k'=2)}_{\alpha a,a\alpha} &= \frac{1}{2}\left[\delta_{a\alpha}\delta_{a\alpha}+\delta_{\alpha\alpha}\delta_{aa}\right]-\frac{1}{3}\delta_{\alpha a}\delta_{a\alpha}\\ &= \frac{2}{3}\end{aligned} \tag{4.15}$$

The contribution of the scalar mode in the parallel channel is therefore

$$\begin{aligned}X^{(0)}_{\alpha\alpha,\alpha\alpha} &= \left(\frac{b_0}{3}+\frac{2b_2}{3}\right)\Gamma_0\\ &= \frac{8}{15}\Gamma_0\end{aligned} \tag{4.16}$$

The $H^{(C)}$ contribution is in the parallel channel is identical to $H^{(B)}$ as can been seen from (4.6) and (4.7) when $\alpha=\beta=\gamma=\delta$.

The $H^{(A)}$ contribution is

$$X^{(0)}_{\alpha\alpha,\alpha\alpha}=\frac{\Gamma_0}{3} \tag{4.17}$$

We see that $H^{(B,C)}$ in the parallel channel are decreased less than the Cooperon.

4.1.2 Perpendicular channel

For the perpendicular case we have $\alpha=\gamma$ and $\beta=\delta$ (compare with the Cooperon where we had $\alpha=\delta$ and $\beta=\gamma$. The difference is the result of exchanging between β and δ in the new base). The $H^{(B)}$ contribution is given by

$$X^{(0)}_{\alpha\beta,\alpha\beta}\propto\sum_{a,b,k}b^{(k)}\Gamma_0\mathscr{T}^{(k)}_{\alpha b,a\alpha}\mathscr{T}^{(0)}_{a\beta,b\beta}. \tag{4.18}$$

The expression for $\mathscr{T}^{(0)}_{\alpha b,b\beta}$ implies that $a=\beta$ and $b=\beta$. Since $\alpha\neq\beta$ (for the perpendicular case) we must have $a,b\neq\alpha$.

We now need to check that these conditions guarantee that (4.18) gives zero. For that we need to calculate $\mathscr{T}^{(k)}_{\alpha b,a\alpha}$ for $k=0,1,2$.

1. $k=0$

$$\begin{aligned}\mathscr{T}^{(0)}_{\alpha b,a\alpha} &= \frac{1}{3}\delta_{\alpha b}\delta_{a\alpha} \\ &= 0\end{aligned} \tag{4.19}$$

2. $k=1$

$$\mathscr{T}^{(1)}_{\alpha b,a\beta} = \frac{1}{2}\left[\delta_{\alpha a}\delta_{b\beta}-\delta_{\alpha\beta}\delta_{ab}\right]=0 \tag{4.20}$$

3. $k=2$

The tensor projector is composed of terms from both the $k=0$ and $k=1$ tensors, which give

$$\mathscr{T}^{(2)}_{\alpha b,a\beta} = \frac{1}{2} \tag{4.21}$$

We see the $H^{(B)}$ does not contribute to the perpendicular channel. We follow the same calculation for $H^{(C)}$. For $H^{(C)}$ we have

$$X^{(0)}_{\alpha\beta,\alpha\beta} \propto \sum_{a,b,k} b^{(k)}\Gamma_0 \mathscr{T}^{(k)}_{\beta b,a\beta}\mathscr{T}^{(0)}_{\alpha a,\alpha b}. \tag{4.22}$$

which requires $a=b=\alpha\neq\beta$

1. $k=0$

$$\mathscr{T}^{(0)}_{\alpha b,a\alpha} = 0 \tag{4.23}$$

2. $k=1$

$$\mathscr{T}^{(1)}_{\alpha b,a\beta} = \frac{1}{2}\left[\delta_{\alpha a}\delta_{b\beta}-\delta_{\alpha\beta}\delta_{ab}\right]=0 \tag{4.24}$$

3. $k=2$

Just as for $H^{(B)}$ this term is zero.

The outcome of the above calculations shows that the contribution of $H^{(B,C)}$ to the intensity in the parallel channel is multiplied by a factor $8/15$ due to the polarization

$$\begin{aligned}X^{(0)}_{\alpha\alpha,\alpha\alpha} &\propto \left(\frac{b_0}{3}+\frac{2b_2}{3}\right)\Gamma_0 \\ &= \frac{8}{15}\Gamma_0.\end{aligned} \tag{4.25}$$

while contributing nothing in the perpendicular channel, like the Cooperon.

That the structure factor is attenuated differently for $H^{(B,C)}$ compared to $H^{(A)}$ raises a doubt about the correctness of (1.84) for the polarized problem. However we only calculated in this section the effect of the polarization degrees of freedom on the structure factor. We did not calculate the total contribution of the Hikami boxes to the scattered intensity which depends also on the scattering angle. This will be done in the following chapter.

Chapter 5

Contribution of $H^{(B)}$ and $H^{(C)}$ to the scattered intensity

The results of the last two chapters are now used to verify that the two additional Hikami boxes, $H^{(B)}$ and $H^{(C)}$ restore energy conservation for the polarized coherent backscattering. The result of the calculation is then compared to experimental measurements of the scattering intensity.

5.1 The Hikami box diagram

We have shown in chapter 4 that when the polarization is taken into consideration the contribution to the intensity of $H^{(B,C)}$ can be written as a superposition of the contribution of each mode. Only the scalar mode has a contribution which is not strongly attenuated in the parallel, and the effect of polarization is to simply multiply it by a factor $8/15$. In the perpendicular channel there is no contribution to the scattered intensity by $H^{(B,C)}$. In this part we calculate the contribution of the scalar mode in the parallel channel and show that it restores the normalization of the probability.

Let us write the expressions for the different constituents of the diagram which appears in figure (5.1). First there is the incoming wave (for simplicity we take the incoming wave to be normal to the interface)

$$\bar{\psi}_i(\mathbf{r}_1) = \sqrt{\frac{cI_0}{4\pi}} e^{-\frac{z_1}{2l_{pol}}} e^{ik_i z_1} \tag{5.1}$$

$$\bar{\psi}_i^*(\mathbf{r}) = \sqrt{\frac{cI_0}{4\pi}} e^{-\frac{z}{2l_{pol}}} e^{-ik_i z} \tag{5.2}$$

The wave amplitude in (5.1) follows a series of scattering events from $\mathbf{r_1}$ to $\mathbf{r}_2$ which is represented by the structure factor, and finally emerges from the scattering medium, where the exit term is

$$\begin{aligned} \overline{G}^R(\mathbf{r}_2, \mathbf{R}) &\simeq e^{-\frac{|\mathbf{r}_2' - \mathbf{r}_2|}{2l_{pol}}} e^{-i\mathbf{k}_e \cdot \mathbf{r}_2} \frac{e^{ikR}}{4\pi R} \\ &= e^{-\frac{z_2}{2l_{pol}\cos\alpha}} e^{-i\mathbf{k}_e \cdot \mathbf{r}_2} \frac{e^{ikR}}{4\pi R} \end{aligned} \tag{5.3}$$

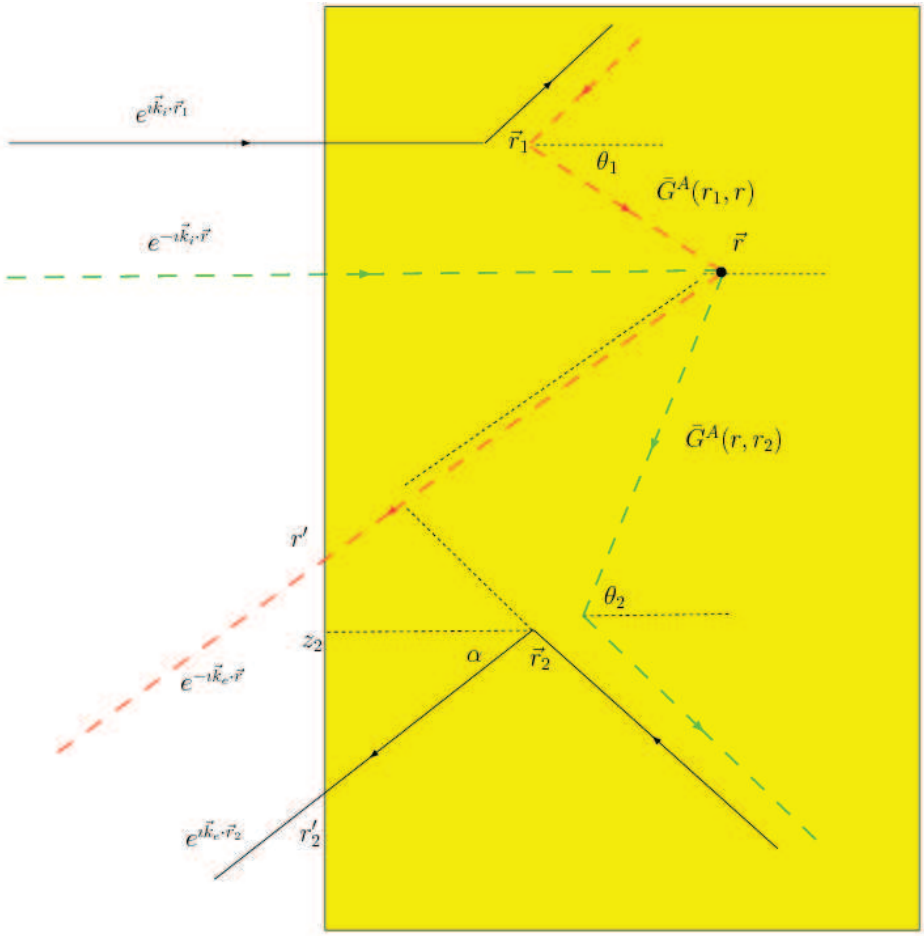

Figure 5.1: Diagram of the Hikami box $H^{(C)}$. The black line represents the incoming and outgoing amplitudes of equations (5.1) *and* (5.3)*. The green line represents the incoming amplitude in equation* (5.2) *which scatters from the additional impurity. The red dashed line represents that amplitude as it leaves given by equation* (5.6)*. The two advanced Green's functions are given by* (5.4) *(in green) and* (5.5) *(in red).*

and the Fraunhoffer approximation has been used to obtain the second equality.

The wave amplitude (5.2) propagates from $\mathbf{r}$ to $\mathbf{r}_2$, scatters along an opposite trajectory to that of the first

amplitude from $\mathbf{r}_2$ to $\mathbf{r}_1$ and finally propagates back to $\mathbf{r}$, from which it leaves the medium towards the detector. The parts $\mathbf{r} \to \mathbf{r}_2$ and $\mathbf{r}_1 \to \mathbf{r}$ are described an advanced Green's functions

$$\overline{G}^A(\mathbf{r},\mathbf{r}_2) = e^{-\frac{|\mathbf{r}-\mathbf{r}_2|}{2l_{pol}}} \frac{e^{ik|\mathbf{r}-\mathbf{r}_2|}}{4\pi|\mathbf{r}-\mathbf{r}_2|} \tag{5.4}$$

$$\overline{G}^A(\mathbf{r}_1,\mathbf{r}) = e^{-\frac{|\mathbf{r}-\mathbf{r}_1|}{2l_{pol}}} \frac{e^{ik|\mathbf{r}-\mathbf{r}_1|}}{4\pi|\mathbf{r}-\mathbf{r}_1|} \tag{5.5}$$

The outgoing amplitude is

$$\overline{G}^A(\mathbf{r},\mathbf{R}) = e^{-\frac{z}{2l_{pol}\cos\alpha}} e^{i\mathbf{k}_e\cdot\mathbf{r}} \frac{e^{-ikR}}{4\pi R} \tag{5.6}$$

We see that the outgoing amplitudes (5.3) and (5.6) have a similar form. They differ only by the attenuation due to an additional path covered by the second amplitude[1] and a phase factor. We can now write the expression for the outgoing intensity in the direction $\hat{s}_e$

$$I(R\hat{s}_e) = \frac{4\pi}{c}\frac{4\pi}{l_{pol}} \int d\mathbf{r}_1 d\mathbf{r}_2 d\mathbf{r}\, \bar{\psi}_i(\mathbf{r}_1)\, \bar{\psi}_i^*(\mathbf{r})\, \overline{G}^A(\mathbf{r},\mathbf{r}_2)\, \Gamma(\mathbf{r}_1,\mathbf{r}_2)\, \overline{G}^A(\mathbf{r}_1,\mathbf{r})\, \overline{G}^R(\mathbf{r}_2,\mathbf{R})\, \overline{G}^A(\mathbf{r},\mathbf{R}) \tag{5.7}$$

where the $\frac{4\pi}{l_{pol}} = \gamma_e$ comes from (1.80)

Inserting the explicit expressions into (5.7) we have, once replacing the structure factor with the diffusion probability (1.56)

$$\begin{aligned} I &= \frac{4\pi c I_0}{l_{pol}^2}\frac{4\pi}{l_{pol}} \int d\mathbf{r}_1 d\mathbf{r}_2 d\mathbf{r} e^{-\frac{z+z_1}{2l_{pol}}} e^{i\mathbf{k}\cdot(\mathbf{r}_1-\mathbf{r})} e^{-\frac{|\mathbf{r}-\mathbf{r}_2|}{2l_{pol}}} \frac{e^{ik|\mathbf{r}-\mathbf{r}_2|}}{4\pi|\mathbf{r}-\mathbf{r}_2|} p_d(\mathbf{r}_1,\mathbf{r}_2)\, e^{-\frac{|\mathbf{r}-\mathbf{r}_1|}{2l_{pol}}} \frac{e^{ik|\mathbf{r}-\mathbf{r}_1|}}{4\pi|\mathbf{r}-\mathbf{r}_1|} \\ &\quad \times e^{-\frac{z_2}{2l_{pol}\cos\alpha}} e^{-i\mathbf{k}_e\cdot\mathbf{r}_2} \frac{e^{ik_eR}}{4\pi R} e^{-\frac{z}{2l_{pol}\cos\alpha}} e^{i\mathbf{k}_e\cdot\mathbf{r}} \frac{e^{-ik_eR}}{4\pi R} \\ &= \frac{cI_0}{l_{pol}^3R^2} \int d\mathbf{r} e^{-\frac{z}{2l_{pol}}\left(\frac{\mu+1}{\mu}\right)} \int d\mathbf{r}_1 d\mathbf{r}_2 e^{-\frac{z_1}{2l_{pol}}} e^{i\mathbf{k}\cdot(\mathbf{r}_1-\mathbf{r})} e^{-\frac{|\mathbf{r}-\mathbf{r}_1|}{2l_{pol}}} \frac{e^{ik|\mathbf{r}-\mathbf{r}_1|}}{4\pi|\mathbf{r}-\mathbf{r}_1|} p_d(r_1,r_2) \\ &\quad \times e^{-\frac{|\mathbf{r}-\mathbf{r}_2|}{2l_{pol}}} \frac{e^{ik|\mathbf{r}-\mathbf{r}_2|}}{4\pi|\mathbf{r}-\mathbf{r}_2|} e^{-\frac{z_2}{2l_{pol}\mu}} e^{-i\mathbf{k}_e\cdot(\mathbf{r}_2-\mathbf{r})} \end{aligned} \tag{5.8}$$

with p_d given in cylindrical coordinates by

$$p_d(\rho,z_1,z_2) = \frac{1}{4\pi D}\left[\frac{1}{\sqrt{\rho^2+(z_1-z_2)^2}} - \frac{1}{\sqrt{\rho^2+(z_1+z_2+2z_0)^2}}\right] \tag{5.9}$$

5.2 The approximated 1D problem

The diffusion term makes the integration difficult, and we must resort to an approximation of the original expression. Let us recall that for weak disorder $l_{pol} \gg \lambda$. As a result we notice the complex exponential terms in (5.8) oscillate rapidly when $\mathbf{r}-\mathbf{r}_1$ or $\mathbf{r}-\mathbf{r}_2$ are of order of l_{pol}. We can use this to our advantage to simplify the calculations.

[1] This additional path can be seen in figure (5.1) marked with a dotted line along the red dashed line. The length of the path is $|\mathbf{r}-\mathbf{r}_2|\cos(\theta_2-\alpha) = \mathbf{k}_e\cdot(\mathbf{r}_2-\mathbf{r})$.

1. We take the z coordinate of the points $\mathbf{r}, \mathbf{r}_1$ and $\mathbf{r}_2$ to be identical in p_d. The reasoning behind is that these coordinates can not be to different from one another (on a scale of a wave length) or the complex exponentials in 5.8 will oscillate rapidly, giving zero after integration. Since the diffusion probability p_d varies much slower with z, z_1, z_2 compared to the other terms in the integrand, these coordinates may as well be taken as identical.

2. Looking at (5.8) we see that the scattered intensity in (5.8) varies much slower with ρ compared to z. We choose therefore to take ρ as a constant of value rl_{pol}. r is a fitting parameter which we expect to be of order of 1.

With the above approximations we end up with a much simpler integral. The approximated diffusion probability[2] p_d depends only on one coordinate

$$p'_d(z) = \frac{1}{4\pi D l_{pol}} \left[\frac{1}{r} - \frac{1}{\sqrt{r^2 + 4\left(\frac{z}{l_{pol}} + \frac{2}{3}\right)^2}} \right]. \tag{5.10}$$

We can solve the rest of the integral following the calculation in [16]. The integral in (5.8) has been decoupled now, and contains a product of integrals, each depending on a single variable.

$$\begin{aligned} I &= \frac{cI_0}{R^2 l_{pol}^3} \int \mathrm{d}z e^{-\frac{z}{2l_{pol}}\left(\frac{\mu+1}{\mu}\right)} p'_d(z) \\ &\times \int \mathrm{d}\mathbf{r}_1 e^{i\mathbf{k}\cdot(\mathbf{r}_1-\mathbf{r})} \overline{G}^A(\mathbf{r}, \mathbf{r}_1) e^{-\frac{z_1}{2l_{pol}}} \int d\mathbf{r}_2 e^{i\mathbf{k}_e\cdot(\mathbf{r}-\mathbf{r}_2)} \overline{G}^A(\mathbf{r}_2, \mathbf{r}) e^{-\frac{z_2}{2l_{pol}\mu}} \end{aligned} \tag{5.11}$$

We can see that the last couple of integral differs only by the value of μ, which is the cosine of the entering\leaving angle. Changing variables $r = |r_1 - r|$ and introducing the angle θ_1 in figure (5.1) the integral for r_1 is

$$J_1(r) = -\int_0^\infty 2\pi r^2 \mathrm{d}r \int_0^\pi \frac{e^{ikr(\cos\theta_1 - 1)}}{4\pi r} e^{-\left[\frac{z+r(1+\cos\theta_1)}{2l_{pol}}\right]} \sin\theta_1 \mathrm{d}\theta_1 \tag{5.12}$$

For a fixed r the integration must be split into two parts

$$j_A = -\frac{1}{2}\int_0^z r\mathrm{d}r \int_0^\pi e^{ikr(\cos\theta_1 - 1)} e^{-\left[\frac{z+r(1+\cos\theta_1)}{2l_{pol}}\right]} \sin\theta_1 \mathrm{d}\theta_1 \tag{5.13}$$

$$j_B = \frac{1}{2}\int_z^\infty r\mathrm{d}r \int_0^\beta e^{ikr(\cos\theta_1 - 1)} e^{-\left[\frac{z+r(1+\cos\theta_1)}{2l_{pol}}\right]} \sin\theta_1 \mathrm{d}\theta_1 \tag{5.14}$$

where z is the distance of the added impurity from the interface and β is defined through the equality

$$z + r\cos\beta = 0. \tag{5.15}$$

[2] Strictly speaking $p'_d(z)$ is not a true diffusion probability as it is not normalized. We resort to using it to simplify the calculations.

The purpose of this splitting is to make sure the end points of the structure factor are kept inside the bulk when $r > z$. The two integrals, $j_{A,B}$ are easily calculated

$$j_A = -e^{-\frac{z}{2l_{pol}}} \frac{\left[l_{pol}\left(1-e^{-\frac{z}{l_{pol}}}\right)+\frac{i}{k}\left(1-e^{-2ikz}\right)\right]}{2\left(ik+\frac{1}{2l_{pol}}\right)}. \tag{5.16}$$

$$j_B = -e^{-\frac{z}{2l_{pol}}} \frac{\left[l_{pol}e^{-\frac{z}{l_{pol}}}+\frac{i}{k+\frac{i}{2l_{pol}}}e^{-2ikz}\right]}{2\left(ik+\frac{1}{2l_{pol}}\right)}. \tag{5.17}$$

Combining the two terms, and neglecting the fast oscillating exponentials we get

$$J_1(r) = \frac{e^{-\frac{z}{2l_{pol}}}}{2}\frac{l_{pol}+\frac{i}{2k}}{ik+\frac{1}{2l_{pol}}} \tag{5.18}$$

which in the limit $kl_{pol} \gg 1$ gives

$$J_1 = e^{-\frac{z}{2l_{pol}}}\frac{il_{pol}}{2k} \tag{5.19}$$

and similarly

$$J_2 = e^{-\frac{z}{2l_{pol}\mu}}\frac{il_{pol}}{2k} \tag{5.20}$$

Our Notice that both results are imaginary, and therefore their product is negative which is expected, since the $H^{(B,C)}$ contribution is suppose to cancel out with the positive Cooperon. Inserting (5.19) and (5.20) into (5.11) we have the following expression for the contribution of $H^{(C)}$ to the albedo

$$\begin{aligned}
\alpha^{(C)} &= -\frac{c}{4k^2}\frac{1}{l_{pol}}\frac{1}{S}\int_s \mathrm{d}\mathbf{r}e^{-\frac{z}{l_{pol}}\left(\frac{\mu+1}{\mu}\right)}p'_d(\mathbf{r}) \\
&\approx -\frac{c}{16\pi k^2 l_{pol}^2 D}\int \mathrm{d}z e^{-\frac{z}{l_{pol}}\left(\frac{\mu+1}{\mu}\right)}p'_d(z) \\
&= -\frac{3}{4k^2 l_{pol}^2}\int_0^\infty \frac{dz}{l_{pol}}\left(\frac{1}{r}-\frac{1}{\sqrt{r^2+4\left(\frac{z}{l_{pol}}+\frac{2}{3}\right)^2}}\right)e^{-\frac{z}{2l_{pol}}\left(\frac{\mu+1}{\mu}\right)}
\end{aligned} \tag{5.21}$$

We wish to show that the inclusion of the the two additional contributions to the albedo, namely $H^{(B)}$ and $H^{(C)}$ restore energy conservation. Our approach is to minimize the total coherent contribution given by

$$\alpha = \int d\mu\left(a\alpha_A + b\alpha_B + b\alpha_C\right) \tag{5.22}$$

where a and b are the prefactors found in the previous chapter. Numerically[3] we find the parameters r, kl_{pol} which give the best fit to the experimental results

[3] Using the "Mathematica" software by Wolfram.

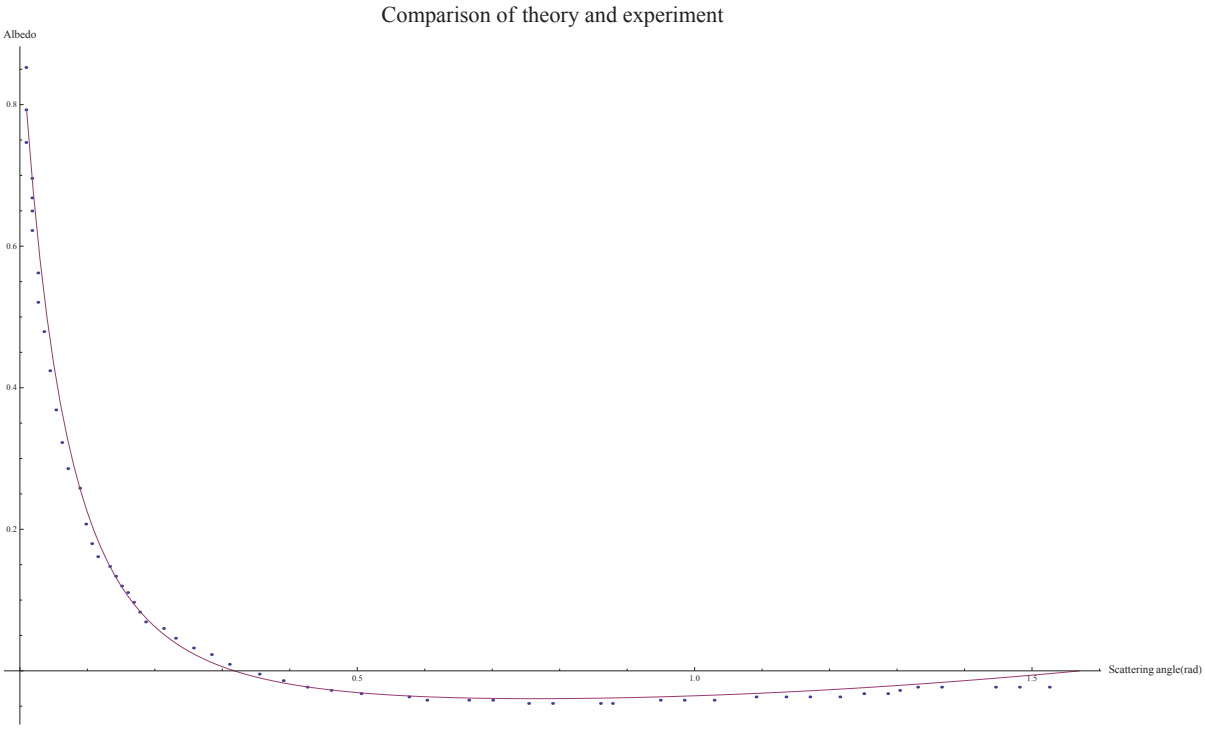

Figure 5.2: The plot above shows the theoretical coherent contribution to the albedo (the solid line) for $kl_{pol} = 6.7$ and $r = 0.9$ compared to the experimental result of [7] (dots).

$$\begin{aligned} kl_{pol} &= 6.7 \\ r &= 0.9 \end{aligned} \tag{5.23}$$

A plot of the fitting is shown in figure (5.2).

The coherent contribution to the albedo (2.16) with $kl_{pol} = 6.7$ was calculated[4] to be 0.0028 compared to 0.0094 of the Cooperon alone. We therefore see a reduction of about 70% in the coherent contribution to the albedo when including all three crossed diagrams. A similar calculation performed for the scalar problem gave a reduction of only 60% (from 0.01 to 0.004). The detailed calculation is given in appendix B. We see that when we include the polarization the coherent contribution is smaller by 30% compared to the scalar model.

[4] In [7] the total coherent contribution was calculated to be 0.005 ± 0.007 with a transport mean free path of 2.5 ± 0.2.

Chapter 6

Conclusion

In this work we have shown the existence of energy conservation in the theory of coherent back scattering. This seemingly violation was primarily due to the inclusion of the Cooperon alone contribution to the scattered intensity. This contribution which is positive for all angles needs to be compensated for, as in its absence, the remaining classical contribution is normalized. We proved that one can not include just the Cooperon since there are other terms of the same order in the perturbation series as the Cooperon. These additional terms along with the Cooperon constitute a dressed Cooperon, whose contribution over all angles vanishes as should.

In order to compare the theory to experimental results we also included the effects of polarization. The polarization distributes the classical contribution to the intensity evenly between all directions. The coherent intensity subsists only in the parallel channel (where the outgoing polarization is parallel to the incoming one), albeit attenuated by a factor of $1/3$ for the Cooperon and $8/15$ for the two other crossed diagrams.

The contributions of the additional crossed diagrams, $H^{(B,C)}$ were then calculated. In order to overcome the difficulties associated with the integration we suggested using a single z coordinate for the point $\mathbf{r}, \mathbf{r}_1$ and $\mathbf{r}_2$. That, and ignoring the propagation parallel to the surface of the medium (the ρ coordinate) allowed us to turn a multivariate integration into a product of single variable integrals which is easily obtained.

The expression for the albedo included a fitting parameter whose value should depend on the polarized mean free path in the problem. This parameter, together with the polarized mean free path were obtained by looking for the best fit of the theoretical model to an experimental result. The outcome showed that the total coherent contribution was smaller when polarization was included in the calculation, compared to the scalar model, although not by much. Better result would be probably obtained if a full analytic solution of (5.8) could be found.

Appendix A

Disorder and averaging

A random medium is much harder to characterize than a lattice. By definition there is no internal structure or order which will allow us to describe the medium using a simple set of mathematical relations. This is not uncommon. Even lattice models which are used to describe most systems in a condensed phase are a simple idealization, as one is well aware of the existence of impurities, defects and other elements which break the periodic structure used by the model. However, unlike theories which involve lattices, in a random medium we cannot treat the random elements of the potential as a perturbation, simply because there is no internal structure to begin with. All we can do is average over different realizations of the system.

What is a realization? Consider the different trajectories of the diffusing radiation inside the medium. Each ends up at a certain scatterer near the boundary of the medium (the probability for the last scatterer to be located deep within the bulk decreases exponentially). The scatterer can be considered as a source of a spherical wave. For our purpose, a realization is an ensemble of such sources whose phases are random. The randomness comes from the fact that trajectories which end up at different scatterers most likely have different lengths. The accumulated phase with which the waves leave the medium depends on the length of those trajectories. For two trajectories, whose lengths are of order of several mean free path and more, to have the same phase would require them to be identical to an accuracy finer than a wave length. In the limit of $\lambda \ll l_e$ which we employ is it is very unlikely. Each such realization is characterized by a detected image called a speckle pattern [17]. Each speckle pattern is unique and has one to one correspondence to its generating realization.

As a result of the motion of the scatterers, a moment later we will have a different set of scatterers which scatter the wave toward the detector. This new realization will have a different speckle pattern. After a while the detected intensity will be the sum of the speckle patterns. The image formed in the detector is the average over time. According the ergodic hypothesis it equals the average over the different realizations of the disorder.

In chapter 1 it is demonstrated how the Diffuson and Cooperon are constructed from the ensemble average. It is important to note that these two contributions are mathematical abstracts and not physically measured objects. They are but a way to calculate the average of the true physical objects which are the speckle patterns.

Appendix B

The Mathematica calculation

The following expression are

f : angle dependent $H^{(B+C)}$ contribution
g : The angle dependent Cooperon contribution
F : The total $H^{(B+C)}$ contribution
G : The total Cooperon contribution
h : The total angle dependent coherent contribution
H: The total coherent contribution
c is the parameter kl_{pol}
y is the scattering angle (θ in the text)
r is a fitting parameter

$$f(\mathrm{c\_},\ \mathrm{r\_},\ y) := \mathrm{NIntegrate}\left[-\frac{3\left(\frac{1}{r}-\frac{1}{\sqrt{r^2+4\left(x+\frac{2}{3}\right)^2}}\right)}{2\left((c\,c)\,e^{\frac{x(\cos(y)+1)}{\cos(y)}}\right)},\ \{x,\ 0,\ 100\}\right]$$

$$g(\mathrm{c\_},\ \mathrm{y\_}) := \frac{3\left(\frac{1-e^{-\frac{1}{3}(4\,c\sin(y))}}{c\sin(y)}+\frac{2\cos(y)}{\cos(y)+1}\right)}{(8\,\pi)\left(c\sin(y)+\frac{\cos(y)+1}{2\cos(y)}\right)^2}$$

$$F(\mathrm{c\_},\ \mathrm{r\_}) := \mathrm{NIntegrate}\left[-\frac{3\left(\frac{1}{r}-\frac{1}{\sqrt{r^2+4\left(x+\frac{2}{3}\right)^2}}\right)}{2\left((c\,c)\,e^{\frac{x(\cos(y)+1)}{\cos(y)}}\right)},\ \{x,\ 0,\ 100\},\ \{y,\ 0,\ 1.57\}\right]$$

$$G(\mathrm{c\_}) := \mathrm{NIntegrate}\left[\frac{3\left(\frac{1-e^{-\frac{1}{3}(4\,c\sin(y))}}{c\sin(y)}+\frac{2\cos(y)}{\cos(y)+1}\right)}{(8\,\pi)\left(c\sin(y)+\frac{\cos(y)+1}{2\cos(y)}\right)^2},\ \{y,\ 0,\ 1.57\}\right]$$

$$h(\mathrm{c\_},\ \mathrm{r\_},\ \mathrm{y\_}) := a * f(c,\ r,\ y) + b * g(c,\ y)$$

$$H(\mathrm{c\_},\ \mathrm{r\_}) := a\,F(c,\ r) + b\,G(c)$$

We insert the raw data extracted from reference [7]

```
raw = Table[
  Import["C:\\Users\\mickey\\Desktop\\latestdata.txt", "Table"]]
```

```
{{0.00887, 0.852535}, {0.00887, 0.792627}, {0.00887, 0.746544},
 {0.01774, 0.695853}, {0.01774, 0.668203}, {0.01774, 0.64977},
 {0.01774, 0.62212}, {0.02661, 0.562212}, {0.02661, 0.520737},
 {0.03548, 0.479263}, {0.04435, 0.423963}, {0.05322, 0.368664},
 {0.06209, 0.322581}, {0.07096, 0.285714}, {0.088701, 0.258065},
 {0.097571, 0.207373}, {0.106441, 0.179724}, {0.115311, 0.16129},
 {0.133051, 0.147465}, {0.141921, 0.133641}, {0.150791, 0.119816},
 {0.159661, 0.110599}, {0.168531, 0.096774}, {0.177401, 0.082949},
 {0.186271, 0.069124}, {0.212881, 0.059908}, {0.230621, 0.046083},
 {0.257232, 0.032258}, {0.283842, 0.023041}, {0.310452, 0.009217},
 {0.354802, -0.004608}, {0.390282, -0.013825},
 {0.425763, -0.023041}, {0.461243, -0.02765}, {0.505593, -0.032258},
 {0.576554, -0.036866}, {0.603164, -0.041475},
 {0.665254, -0.041475}, {0.700734, -0.041475},
 {0.753955, -0.046083}, {0.789435, -0.046083},
 {0.860395, -0.046083}, {0.878136, -0.046083},
 {0.949096, -0.041475}, {0.984576, -0.041475}, {1.02893, -0.041475},
 {1.09102, -0.036866}, {1.13537, -0.036866}, {1.17085, -0.036866},
 {1.2152, -0.036866}, {1.25068, -0.032258}, {1.28616, -0.032258},
 {1.3039, -0.02765}, {1.33051, -0.023041}, {1.36599, -0.023041},
 {1.44582, -0.023041}, {1.4813, -0.023041}, {1.52565, -0.023041}}
```

We create a list of values from the theoretical expression for the angle dependedn coherent contribution with the following values for c and r

```
c = 6.7
r = 0.9
```

```
6.7
```

```
0.9
```

To ensure the theoretical and expreimental data have the same scale we multiply the theoretical expression by 3 (so the polarization prefactors in h(c, r, y) are now b=1 for $H^{(A)}$ and a=1.6 for $H^{(B+C)}$).

```
a = 1.6
```

```
1.6
```

$$\text{fit} = \text{Table}\left[\left\{y,\ \frac{1}{7}(8\pi)\,a\ \text{NIntegrate}\left[-\frac{3\left(\frac{1}{r}-\frac{1}{\sqrt{r^2+4\left(x+\frac{2}{3}\right)^2}}\right)}{2\left((c\,c)\,e^{\frac{x(\cos(y)+1)}{\cos(y)}}\right)},\ \{x,\ 0,\ 100\}\right]+\right.$$

$$\left.\frac{(8\pi)\left(3\left(\frac{1-e^{-\frac{1}{3}(4c\sin(y))}}{c\sin(y)}+\frac{2\cos(y)}{\cos(y)+1}\right)\right)}{7\left((8\pi)\left(c\sin(y)+\frac{\cos(y)+1}{2\cos(y)}\right)^2\right)}\right\},\ \{y,\ 0.01,\ 1.57,\ 0.01\}\Bigg]$$

```
{{0.01, 0.791954}, {0.02, 0.675464},
 {0.03, 0.5798}, {0.04, 0.500446}, {0.05, 0.434024},
 {0.06, 0.377973}, {0.07, 0.33032}, {0.08, 0.289532},
 {0.09, 0.254402}, {0.1, 0.223972}, {0.11, 0.197472},
 {0.12, 0.174283}, {0.13, 0.153897}, {0.14, 0.135899},
 {0.15, 0.119946}, {0.16, 0.105753}, {0.17, 0.0930812},
 {0.18, 0.0817313}, {0.19, 0.0715337}, {0.2, 0.0623446},
 {0.21, 0.0540418}, {0.22, 0.0465204}, {0.23, 0.0396903},
 {0.24, 0.0334737}, {0.25, 0.0278032}, {0.26, 0.0226203},
 {0.27, 0.017874}, {0.28, 0.0135197}, {0.29, 0.00951801},
 {0.3, 0.00583462}, {0.31, 0.00243907}, {0.32, -0.000695534},
 {0.33, -0.00359306}, {0.34, -0.00627471}, {0.35, -0.0087594},
 {0.36, -0.011064}, {0.37, -0.0132036}, {0.38, -0.0151918},
 {0.39, -0.0170407}, {0.4, -0.0187614}, {0.41, -0.0203636},
 {0.42, -0.0218564}, {0.43, -0.0232478}, {0.44, -0.0245452},
 {0.45, -0.0257552}, {0.46, -0.0268839}, {0.47, -0.0279368},
 {0.48, -0.0289189}, {0.49, -0.0298349}, {0.5, -0.0306889},
 {0.51, -0.0314849}, {0.52, -0.0322263}, {0.53, -0.0329163},
 {0.54, -0.0335581}, {0.55, -0.0341543}, {0.56, -0.0347074},
 {0.57, -0.0352198}, {0.58, -0.0356937}, {0.59, -0.0361311},
 {0.6, -0.0365337}, {0.61, -0.0369033}, {0.62, -0.0372415},
 {0.63, -0.0375497}, {0.64, -0.0378294}, {0.65, -0.0380817},
 {0.66, -0.0383078}, {0.67, -0.0385089}, {0.68, -0.038686},
 {0.69, -0.0388399}, {0.7, -0.0389717}, {0.71, -0.039082},
 {0.72, -0.0391718}, {0.73, -0.0392416}, {0.74, -0.0392921},
 {0.75, -0.0393241}, {0.76, -0.039338}, {0.77, -0.0393345},
 {0.78, -0.0393139}, {0.79, -0.0392768}, {0.8, -0.0392237},
 {0.81, -0.0391549}, {0.82, -0.0390709}, {0.83, -0.0389719},
 {0.84, -0.0388584}, {0.85, -0.0387307}, {0.86, -0.038589},
 {0.87, -0.0384336}, {0.88, -0.0382648}, {0.89, -0.0380828},
 {0.9, -0.0378878}, {0.91, -0.0376801}, {0.92, -0.0374598},
 {0.93, -0.0372271}, {0.94, -0.0369823}, {0.95, -0.0367253},
 {0.96, -0.0364565}, {0.97, -0.0361759}, {0.98, -0.0358836},
 {0.99, -0.0355797}, {1., -0.0352645}, {1.01, -0.0349378},
 {1.02, -0.0345999}, {1.03, -0.0342509}, {1.04, -0.0338907},
 {1.05, -0.0335195}, {1.06, -0.0331374}, {1.07, -0.0327443},
 {1.08, -0.0323403}, {1.09, -0.0319256}, {1.1, -0.0315},
 {1.11, -0.0310638}, {1.12, -0.0306168}, {1.13, -0.0301592},
 {1.14, -0.0296909}, {1.15, -0.029212}, {1.16, -0.0287225},
 {1.17, -0.0282225}, {1.18, -0.0277119}, {1.19, -0.0271908},
 {1.2, -0.0266592}, {1.21, -0.0261172}, {1.22, -0.0255647},
 {1.23, -0.0250018}, {1.24, -0.0244285}, {1.25, -0.0238448},
 {1.26, -0.0232508}, {1.27, -0.0226465}, {1.28, -0.022032},
 {1.29, -0.0214072}, {1.3, -0.0207723}, {1.31, -0.0201273},
 {1.32, -0.0194723}, {1.33, -0.0188074}, {1.34, -0.0181326},
 {1.35, -0.017448}, {1.36, -0.0167537}, {1.37, -0.0160499},
 {1.38, -0.0153366}, {1.39, -0.0146141}, {1.4, -0.0138824},
 {1.41, -0.0131417}, {1.42, -0.0123922}, {1.43, -0.0116341},
 {1.44, -0.0108674}, {1.45, -0.0100925}, {1.46, -0.00930952},
 {1.47, -0.00851851}, {1.48, -0.00771962}, {1.49, -0.00691287},
 {1.5, -0.00609816}, {1.51, -0.0052752}, {1.52, -0.0044434},
 {1.53, -0.0036017}, {1.54, -0.00274827}, {1.55, -0.00188003},
 {1.56, -0.000991807}, {1.57, -0.0000746792}}
```

we plot the raw data vs the theoretical result for c=6.7 and r=0.9 in the polarised case where a=1.6

```
ListPlot[{raw, fit}, PlotRange → All, Joined → {False, True}]
```

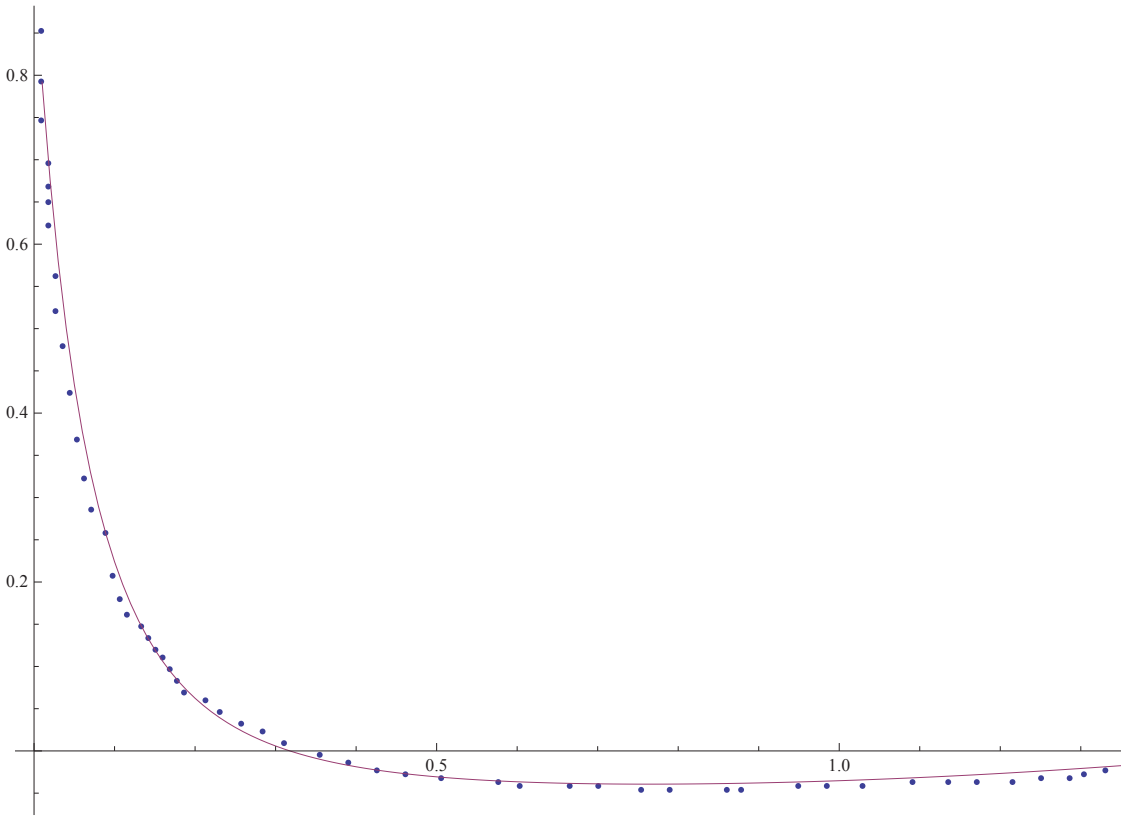


```
raw = Table[Import["C:\\Users\\mickey\\Desktop\\latestdata.txt", "Table"]]
```

In the following 3 lines we calculate the total coherent contribution to the albedo for

1) $H^{(A+B+C)}$ with r = 0.9, c = 6.7, a = 1.6

2) $H^{(A+B+C)}$ with c = 6, r = 0.8, a = 1 (scalar problem where the chosen values give the best fit in this case)

3) The Cooperon contribution for c=6.7 (polarized case)

4) The Cooperon contribution for c=6 (scalar cse)

```
(8 / 15) * F[6.7, 0.9] + (1 / 3) * G[6.7]
```

```
0.0027999
```

```
(1 / 3) * (F[6., 0.8] + G[6.])
```

```
0.00424565
```

```
(1 / 3) * G[6.7]
```

```
0.00942122
```

```
(1 / 3) * G[6]
```

```
0.0104269
```

Appendix C

Experimental setup and various results

Attempts to observe coherent back scattering have met success to various degrees since the 1980's. The main difficulty is the need to place the source of the radiation and the detector on the same line. One possible setup which is used to overcome this involves placing a beam splitter in the path of the wave. This allows the scattered wave to be directed to a detector located away from the line of the incoming wave.

The setup is composed from the following main parts:

1. A coherent source of radiation
2. A combination of a pinhole and converging lens.
3. A beam splitter which let some half of the wave propagate forward, while deflecting the other half.
4. A quarter wave plate which turns a linear polarization into a circular one.
5. A sample of material with proper qualities.
6. A polarizer.
7. Detector.

The purpose of the pinhole and the lens is to expand the emitted coherent beam in order to form an approximated plane wave. A more important role plays the quarter wave plate. It's used to filter out the single scattered contribution to the outgoing wave. This contribution to the scattered intensity does not contribute to the Diffuson or the crossed diagrams, and is much greater than of the later ones, masking their signal. The plate turns the incoming linearly polarized wave into a circular polarized one. Such a wave has its phase reversed when going through a single scattering reflection. Upon passing the second time through the plate it becomes again a linearly polarized wave, but with a polarization perpendicular to that which it had before. Placing a properly aligned polarizer will then block the single scattered wave. After the light pass through the plate, the beam splitter reflects part of it to a focusing lens and a detector. The use of a beam splitter has its own problems, as it can alter the polarization if the wave, which will make it difficult to block the single scattering background. The results of an experiment carried with the above setup are shown in figure (C.2).

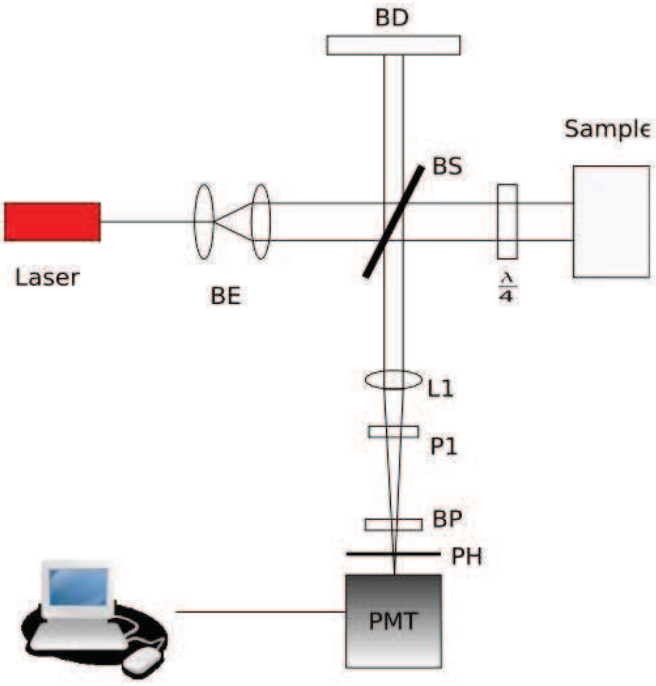

Figure C.1: A typical experimental setup

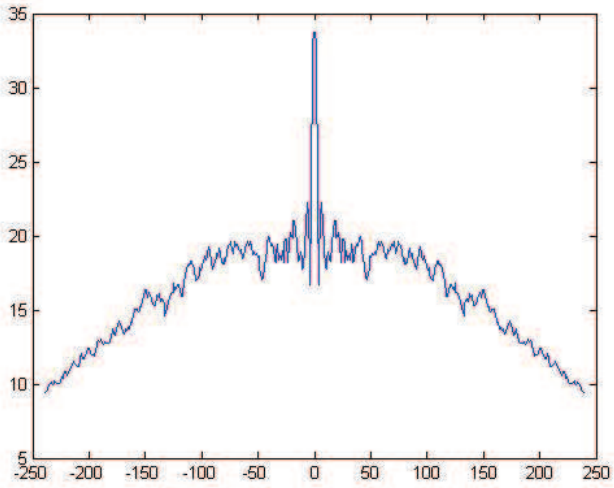

Figure C.2: Result of coherent back scattering measurement performed by the author with the setup described in the appendix. The classical intensity is represented by the arc with its maximal value at about 20 (in arbitrary units). The peak in the middle is the non classical contribution, shown to reach a maximal intensity at zero angle with an enhancement of about 70% with respect to the maximal intensity of the classical contribution. The source of the fluctuations is the measuring apparatus which includes an opaque screen before the detector. The detected beam passes through a rectangle opening in the screen which results in a convolution between the beam and a sinc function.

Bibliography

[1] E. Akkermans and R. Maynard. Weak localization of waves. *J. Physique Lett.*, 46:1045–1053, 1985.

[2] R. Maynard, P.E. Wolf, G. Maret, and E. Akkermans. Coherent backscattering of light by disordered media: Analysis of the peak line shape. *Phys. Rev. Lett*, (56):1471–1474, 1986.

[3] E. Akkermans, P.E. Wolf, R. Maynard, and G. Maret. Theoretical study of the coherent backscattering of light by disordered media. *J. de Physique*, (49):77–98, 1988.

[4] G. Maret and E. Akkermans R. Maynard, P. E. Wolf. Optical coherent backscattering by random media: An experimental study. *J. de Physique*, (49):63–75, 1988.

[5] M.P. van Albada and A. Lagendijk. Observation of weak localization of light in a random medium. *Phys. Rev. Lett.*, 55(24):2692–2695, Dec 1985.

[6] P. Wolf and G. Maret. Weak localization and coherent backscattering of photons in disordered media. *Phys. Rev. Lett.*, 55(24):2696–2699, Dec 1985.

[7] S. Fiebig, C. M. Aegerter, W. Bührer, M. Störzer, E. Akkermans, G. Montambaux, and and G. Maret. Conservation of energy in coherent backscattering of light. *Europhys. Lett.*, (81):64004, 2008.

[8] E. Akkermans and G. Montambaux. *Mesoscopic Physics of Electrons and Photons*. Cambridge, 2007.

[9] A. A. Golubentsev. The suppression of interference effects in the multiple scattering of light. *Zhurnal Eksperimental noi i Teoreticheskoi Fiziki (Journal of experimental and theoretical physics)*, 86:47–59, January 1984.

[10] M. C. W. van Rossum and Th. M. Nieuwenhuizen. Multiple scattering of classical waves: Microscopy, mesoscopy, and diffusion. *Rev. Mod. Phys.*, 71(1):313 – 371, January 1999.

[11] S. F. Edwards. A new method for the evaluation of electric conductivity in metals. *Philos. Mag.*, (3):1020, 1958.

[12] C. Cohen-Tannoudji, B. Diu, and F. Laloe. *Quantum mechanics*, volume 1. Wiley-interscience, 1977.

[13] S. Hikami. Anderson localization in a non-linear sigma model representation. *Phys. Rev. B*, (24):2671, 1981.

[14] Diederik S. Wiersma, Meint P. van Albada, Bart A. van Tiggelen, and Ad Lagendijk. Experimental evidence for recurrent multiple scattering events of light in disordered media. *Phys. Rev. Lett.*, 74(21):4193–4196, May 1995.

[15] M. Kushnir. Transport and weak localization of spin S particles: application to the atom-photon systems. Master's thesis, Technion, 2005.

[16] Akkerman E. Private memo.

[17] J. W. Goodman. *Statistical Optics*. Wiley, 1985.

מאפיין זה של הגברת העוצמה עבור פיזור אחורי אושש בניסויים רבים. אך הקופרון מציג בעיה חמורה של הפרת שימור אנרגיה. הדיפוסון יחד עם איבר דרוד-בולצמן מהווים תרומה מנורמלת לעוצמה. כלומר העוצמה המוחזרת המחושבת לפי שני ביטויים אילו שווה לעוצמה הפוגעת בתווך. מאחר והנחת המודל היא שהפיזור אלסטי ואין אובדן בתווך הרי שהתוספת של הקופרון (שהינה חיובית תמיד) מפרה את חוק שימור האנרגיה.

הסיבה לאי השימור נובעת מהאופי ההפרעתי של החישוב. איננו מחשבים בצורה ישירה את העוצמה המתפ-זרת אלא אוספים איברים שונים בטור הפרעתי שמהווה קירוב לתוצאה האמיתית. את האברים בטור ניתן לחלק לסדרים שונים התלויים בחזקה של פרמטר מאפיין (היחס בין המרחק האופייני בין פיזורים לאורך הגל) המופיעה בהם. בקרוב שאנו משתמשים בו פרמטר זה הוא מספר טהור גדול מאד מ 1 והחזקות שליליות.

היקאמי, בעבודתו מסוף שנות ה-70 הראה שקיימים עוד שני אברים בפיתוח ההפרעתי מאותו סדר של הדיפו-סון והקופרון. הקופרון (מסומן ע"י $H^{(A)}$) יחד עם שני האברים הנוספים (שמסומנים ע"י $H^{(B)},H^{(C)}$) מהווים יחד תרומה הנקראת "קופרון לבוש" (dressed Cooperon). תכונתם של שלושת הביטויים (הידועים גם בשם קופסאות היקאמי - Hikami boxes) היא שתרומתם הכוללת בחישוב העוצמה המתפזרת הוא אפס. בכך שאנו כוללים בחישוב את כל התרומות האפשריות בסדר המוביל, ניתן להראות שבסדר זה מתקיים שימור אנרגיה.

הייחוד של עבודה זו הוא שהיא לוקחת בחשבון את הקיטוב של הגל הפוגע. בעבודות קודמות החישובים נעשו עבור גל סקלרי, עבור גל זה איבר האינטראקציה בין הגל למפזר הוא סקלרי. כאשר לוקחים בחשבון את הקי-טוב איבר האינטראקציה הוא טנזור שמתאר את ההסתברות לגל עם קיטוב מסוים להתפזר עם קיטוב אחר. התרומה של הביטויים השונים מחושבת עבור גל מקוטב. במיוחד אנו מראים שקופסאות היקאמי $H^{(B)},H^{(C)}$ תורמות רק לפיזור של הגל המקוטב במקביל לקיטוב של הגל הפוגע בדומה לקופרון (בניגוד לדיפוסון התורם לעוצמה גם לרכיב עם קיטוב בכיוון הניצב לקיטוב הגל הפוגע). התוצאות של החישובים מראות שהתרומה של קופסאות היקמי לפיזור עם קיטוב מקביל מוכפלת בפקטור קבוע (ונבדל עבור הקופרון ושני הביטויים האחרים). בנוסף $H^{(B)},H^{(C)}$ תורמים בצורה שלילית כפי שמתבקש מן הדרישה לקזז את התוספת של הקופרון לעוצמה. בדומה לדיפוסון $H^{(B)},H^{(C)}$ תורמות עבור כל טווח זויות הפיזור, בניגוד לקופרון שתורם רק עבור זויות קטנות. כלומר ההשפעה של קופסאות היקמי היא פילוג מחדש של העוצמה בזויות שונות - הגברה עבור זויות קטנות, והחלשה עבור זויות גדולות יותר.

על מנת לבחון את נכונות החישובים, אנו משווים אותם אל תוצאות ניסיוניות שנתקבלו בשנת 2008. אנו מחשבים מתוך הניסוי את היחס בין המקדמים המספריים המכפילים את התרומה של קופסאות היקמי ומש-ווים לתוצאה התאורטית.

תקציר

עבודה זו עוסקת בשימור אנרגיה בתופעת הפיזור הקוהרנטי לאחור. בהיותו אחד העקרונות הבסיסיים והחשובים ביותר בפיסיקה, התאוריה המתארת את הפיזור הנ"ל לא תהיה שלמה מבלי שתעמוד בדרישה זו. בחיבור זה נדון בפיזור אלסטי לחלוטין מתווך חצי אינסופי כך שכל העוצמה הפוגעת בתווך אמורה להיות מוחזרת דרך פני התווך.

התווך עצמו יכול להיות מורכב מאוסף מפזרים הממוקמים אקראית בתוכו ותופשיים לנוע, או במקרה אחר הוא יכול להיות בעל אינדקס שבירה שמשתנה באופן רציף ואקראי בדומה לאטמוספרה. הגישה המקובלת בטיפול בבעיות כאלו היא בעזרת שיטות הפרעתיות. מאחר והתווך חסר כל מבנה פנימי לא ניתן לתאר אותו ע"י ביטוי מתמטי פשוט ו"חסכני". במקום זאת ניתן להתייחס לקונפיגורציות אפשריות של התווך - כל קונפיגורציה היא אוסף מיקומי המפזרים ברגע נתון. כאשר הגל נכנס לתווך הוא עובר סדרת פיזורים עד שהוא מוחזר מהמפזר האחרון דרך מישור הכניסה אל גלאי. אם נחלק את חזית הגל הפוגע למקטעים קטנים הרי שנוכל לראות שכל מקטע גל, למרות שהוא פוגע באותו זמן כמו שאר המקטעים יעבור מסלול פיזור שונה בדר"כ משאר הגל. הבדל זה נובע מכך שלסידור של המפזרים אין סימטריה להזזות מרחביות. פזת הגל המתפזר תלויה באורך המסלול אותו עבר ולכן מסלולי פיזור שונים יובילו לכך שמקטעי הגל השונים יהיו בעלי פזות שונות. כתוצאה מכך ניתן להסתכל על תופעת הפיזור באופן הבא. נתאר לעצמנו אוסף מפזרים הממוקמים סמוך לפני התווך (הסיכוי שהאור יתפזר החוצה מהתווך קטן מעריכית ככל שהמפזר נמצא עמוק יותר) אשר כל אחד מהם מהווה מקור לגל כדורי יוצא עם פזה אקראית. כתוצאה מכך יגיעו לגלאי גלים עם פזות אקראיות, אשר יצרו תבנית התאבכות. תבנית זו ידועה בשם תבנית כתם (speckle pattern). המיצוע על מספר גדול של תבניות כתם אילו שקול לסכום של גלים עם פזה אקראית. בסכום זה כל אברי ההתאבכות מתבטלים ואני נשארים עם סכום העוצמות בלבד. מסיבה זו רווחה הדעה שתופעות קוהרנטיות לא יכולות להתקיים עבור פוטנציאל אקראי.

מבט עמוק ומדוקדק יותר יראה שאין זאת כך בהכרח. למעשה מתוך אוסף המסלולים השונים בתוך התווך קיימים מסלולים מסוימים שישרדו את המיצוע על פני הקונפיגורציות השונות. כידוע עוצמת הגל היא מכפלה של המשרעת בצמוד המרוכב שלה. לכל משרעת ישנו מסלול משלה, מה שגורר הפרש פזה בין המשרעות ותנודות בעוצמה. כעת תארו לעצמכם קונפיגורציה בה הגל, והצמוד המרוכב שלו נעים לאורך אותה סידרה של מפזרים. הפרש הפזה בין המשרעות יתבטל, והעוצמה תהיה קבועה. ניתן להפריד את התרומה של מסלולים אילו - הידועים בשם דיפוסון (Diffuson) משאר המסלולים. שאר המסלולים יתמצעו לתבנית רקע אחידה שעליה יהיה ניתן להבחין בתרומה של הדיפוסון - כלומר התמונה הנקלטת בגלאי כבר לא תהיה אחידה. עם זאת יש לזכור כי עדיין לא מדובר בתופעה קוהרנטית. זוהי תרומה קלאסית לחלוטין שאינה תלויה בפזה של הגל (כפי שהוסבר הדיפוסון בנוי ממסלולים עבורם לא קיים הפרש פזה בין המשרעות). נשאלת השאלה, לכן, האם קיימת תרומה נוספת קוהרנטית לעוצמה.

עבודתם של אקרמן ומיינארד משנות ה-80 הראתה שאכן קיימת תרומה כזו. תרומה זו נובעת מסימטריה להיפוך זמן שמתקיימת עבור התווך. הודות לסימטריה זו אין חשיבות אם הגל מתקדם לאורך מסלול בכיוון אחד או בכיוון ההפוך. כלומר הגל יכול להתפזר מסדרה של מפזרים בסדר מסוים או בסדר ההפוך. סימטריה זו מאפשרת תרומה נוספת בחישוב העוצמה המתפזרת המתקבלת ע"י כך שאחת המשרעות מתקדמת מסוף המסלול אל תחילתו. כלומר הפיזור הראשון יתרחש במפזר האחרון (ביחס למשרעת האחרת) והפיזור מתוך התווך אל הגלאי יהיה מהמפזר הראשון. יש לשים לב שתרומה זו לעוצמה הידועה בשם קופרון (Cooperon) שונה מהדיפוסון. לדיפוסון יש תלות חלשה מאד בזווית הפיזור ועבור זוויות קטנות הוא כמעט קבוע. עבור הקופרון נשים לב כי משרעת הגל והצמודה שלה מתפזרות החוצה ממפזרים שונים הממוקמים באופן כללי במקומות שונים. דבר זה גורר הפרש פזה בין המשרעות (למרות ששתיהן מגיעות למפזר האחרון שלהן עם אותה פזה) שנעשה משמעותי ככל ששני אתרי הפיזור האחרונים מרוחקים יותר. כתוצאה מכך התרומה של הקופרון קיימת רק עבור זוויות קטנות מאד. כאשר זווית הפיזור הפוכה לזווית הפגיעה (פיזור לאחור) תרומת הקופרון שווה לזו של הדיפוסון, כך שעבור זווית זו עוצמת הפיזור מוכפלת.

המחקר נעשה בהנחיית פרופ' אריק אקרמן בפקולטה לפיסיקה

השפעת הקיטוב על פיזור קוהרנטי לאחור

חיבור על מחקר

לשם מילוי חלקי של הדרישות לקבלת התואר

מגיסטר למדעים בפיסיקה

דיאמנט משה

הוגש לסנט הטכניון - מכון טכנולוגי לישראל

אייר תש"ע חיפה אפריל 2010